



## Historical perspective

# Electro-optic Kerr effect in the study of mixtures of oppositely charged colloids. The case of polymer-surfactant mixtures in aqueous solutions

Hernán A. Ritacco\*

Instituto de Física del Sur (IFISUR), Departamento de Física, Universidad Nacional del Sur (UNS), CONICET. Av. N.L. Alem 1253, B8000CPB Bahía Blanca, Argentina.

## ARTICLE INFO

## Keywords:

Electric birefringence  
 Electro-optic Kerr effect  
 Polymer-surfactant complexes  
 Polyelectrolytes  
 Counterions polarization mechanism

## ABSTRACT

In this review I highlight a very sensitive experimental technique for the study of polymer-surfactant complexation: *The electro-optic Kerr effect*. This review does not intend to be exhaustive in covering the Kerr Effect nor polymer-surfactant systems, instead it aims to call attention to an experimental technique that, even if applied in a qualitative manner, could give very rich and unique information about the structures and aggregation processes occurring in mixtures of oppositely charged colloids. The usefulness of electric birefringence experiments in the study of such systems is illustrated by selected results from literature in hope of stimulating the realization of more birefringence experiments on similar systems. This review is mainly aimed at, but not restricted to, researchers working in polyelectrolyte-surfactant mixtures in aqueous solutions, Kerr effect is a powerful experimental tool that could be used in the study of many systems in diverse areas of colloidal physics.

## 1. Introduction

## 1.1. Kerr effect

Electro-optic Kerr effect refers to the generation of birefringence, i.e. anisotropy in the refraction index, by applying an electric field to an otherwise isotropic material. In Fig. 1 a schematic representation of how birefringence can be generated by electric fields is shown. Birefringence has its origin in an intrinsic anisotropy of the electronic polarizabilities of the molecules that compose the material (see Fig. 1). Molecules in liquid solutions or colloidal particles in suspension adopt, due to thermal agitation, a random orientation that is characterized by an isotropic refractive index, even if the particles are anisotropic (Fig.1a). The application of an external electric field induces order, molecules (or particles) align with the field (Fig. 1b), and the molecule (particle) optical anisotropy is manifested as birefringence: The refractive index ( $n$ ) is different if measured in a direction parallel ( $n_{\parallel}$ ) or perpendicular ( $n_{\perp}$ ) to the electric field. The effect is known as the Kerr effect, in honor of John Kerr, who was the first to observe it. Before starting with a very short overview on the discovery and development of electro-optic Kerr effect, I will first explain the basics of the experiment. In Fig. 2a the typical experimental setup is shown. Light from

any source, today commonly a laser, is polarised and enters a liquid sample placed between parallel plane electrodes connected to a voltage generator. The polarization plane of the incident light is at  $45^{\circ}$  with respect to the applied electric field. In the absence of an electric field, the light passes through the liquid sample retaining its polarization and is extinguished by a second polarizer, the analyser, which is orientated in a crossed position with respect to the first polarizer. In this case both components in which the electric vector of the light can be divided, one parallel,  $E_{\parallel}^0$ , and one perpendicular,  $E_{\perp}^0$ , to the direction of the electric field, are in phase. However, under the influence of an applied external field, the refractive indexes of the liquid become different for the parallel and perpendicular components, as was schematized in Fig. 1, and they emerge from the sample out of phase, producing light elliptically polarised. Thus, the light emergent from the liquid cell has an electric field component perpendicular to the polarization plane of the light emerging from the first polarizer, as a consequence, a portion of the light intensity is transmitted by the analyser and a signal is detected on the photodetector, the birefringence signal. The transmitted light intensity is proportional to the magnitude of the optical anisotropy (an intrinsic property of the molecule, Fig. 1c) and to the intensity of the external electric field applied (the degree of particle orientation increases with the electric field strengths). The features of the

\* Corresponding author.

Email address: hernan.ritacco@uns.edu.ar (H.A. Ritacco)

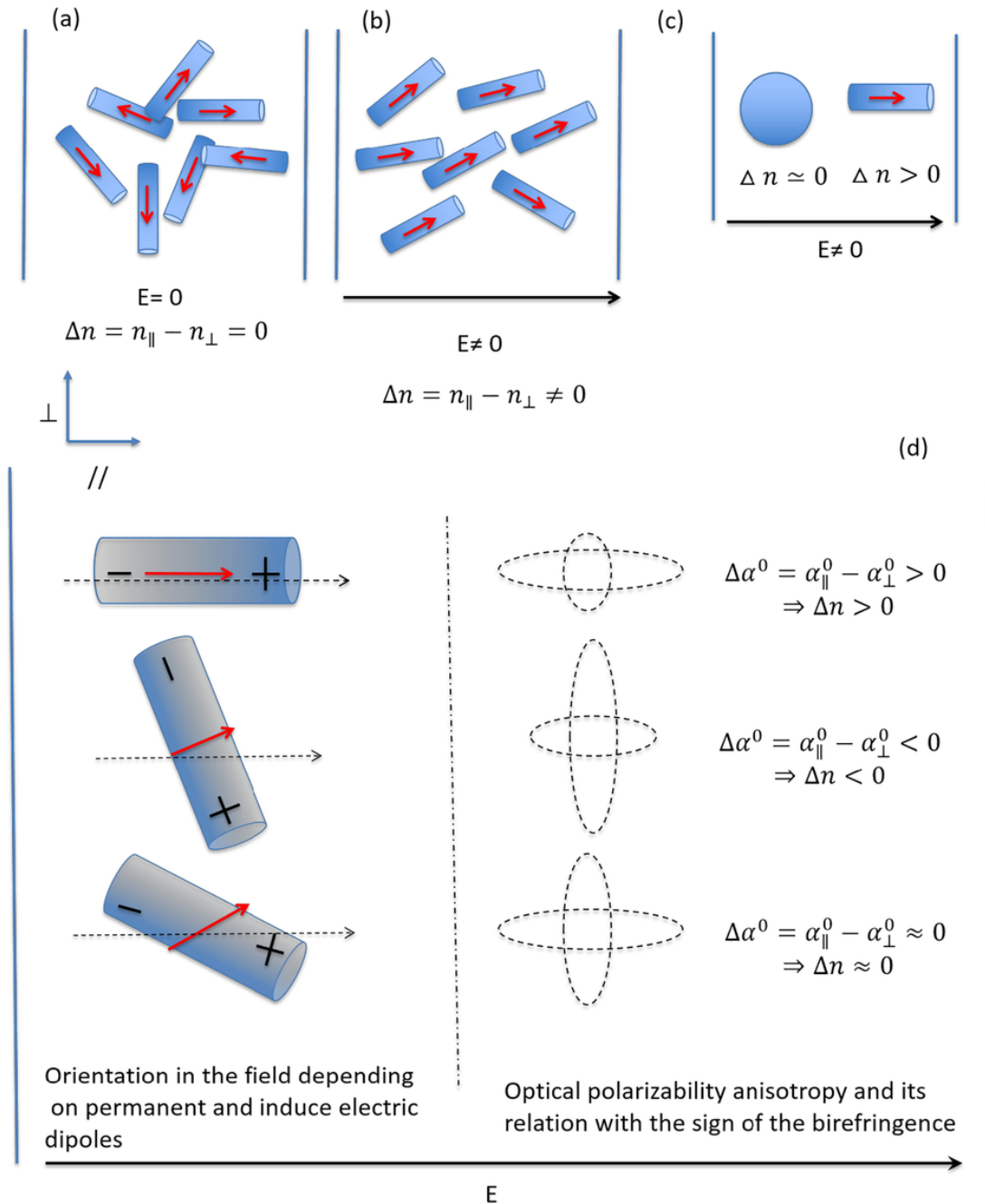


**Fig. 1.** The origin of birefringence is in the intrinsic anisotropy of particles. (a) Schematic representation of anisotropic particles randomly oriented by thermal agitation. In the absence of any orientating field, the particle dispersion is isotropic,  $\Delta n = 0$ ; (b) The same system in a non-zero field: the anisotropic particles orientate in the field due the presence of dipoles. Now the refraction index is different if measured in the direction of the field or perpendicular to it,  $\Delta n \neq 0$ ; (c) Birefringence is a function of particle anisotropy: an ideal rigid sphere is perfectly isotropic and not orientable in a field, thus no birefringence can be induced on it. On the contrary, a cylinder is highly anisotropic and gives place to a non-negligible birefringence when placed in an orientating field; (d) The sign of the birefringence depends on both the total electric dipole moment (represented by a dashed arrow in the figure), resulting from the permanent (arrow) and induced ( $\pm$  signs) dipoles, and the optical polarizability anisotropy of particles (dashed ellipses), this is the anisotropy of the electron polarizability at the frequency of the light source used in the measurement of the refractive index. Because the particle re-orientates itself due to the total electric dipole, the main optical axis can end up falling in any direction between parallel ( $\Delta n > 0$ ) or perpendicular ( $\Delta n < 0$ ) to the direction of the field. The intrinsic optical anisotropy results from the chemical structure of molecules and their conformation in solution (see text for details, Section 2), being the main contribution from  $\pi$ -electrons.

birefringence signal depend on the size and shape of the particles present in the liquid sample (see Section 2) (from now on I will use the word “particle” to refer to not only particles, but also molecules, macromolecules, aggregates or colloids of any kind).

Returning to the discovery and development of electro-optic Kerr effect [2], in 1845 John Kerr published a paper entitled “A new relation between electricity and light” [3] in which he presented for the

first time the observation of birefringence generated by an electric field in several liquids, including carbon disulphide, benzene, paraffin oil and turpentine, among others. The setup used by Kerr was essentially the same as the one described in Fig. 2. He used a candle flame as light source, which was sent through the liquid sample placed in a cell with two electrodes connected to the secondary terminals of a Ruhmkorff induction machine, which was used to produce the electric field. The liq-

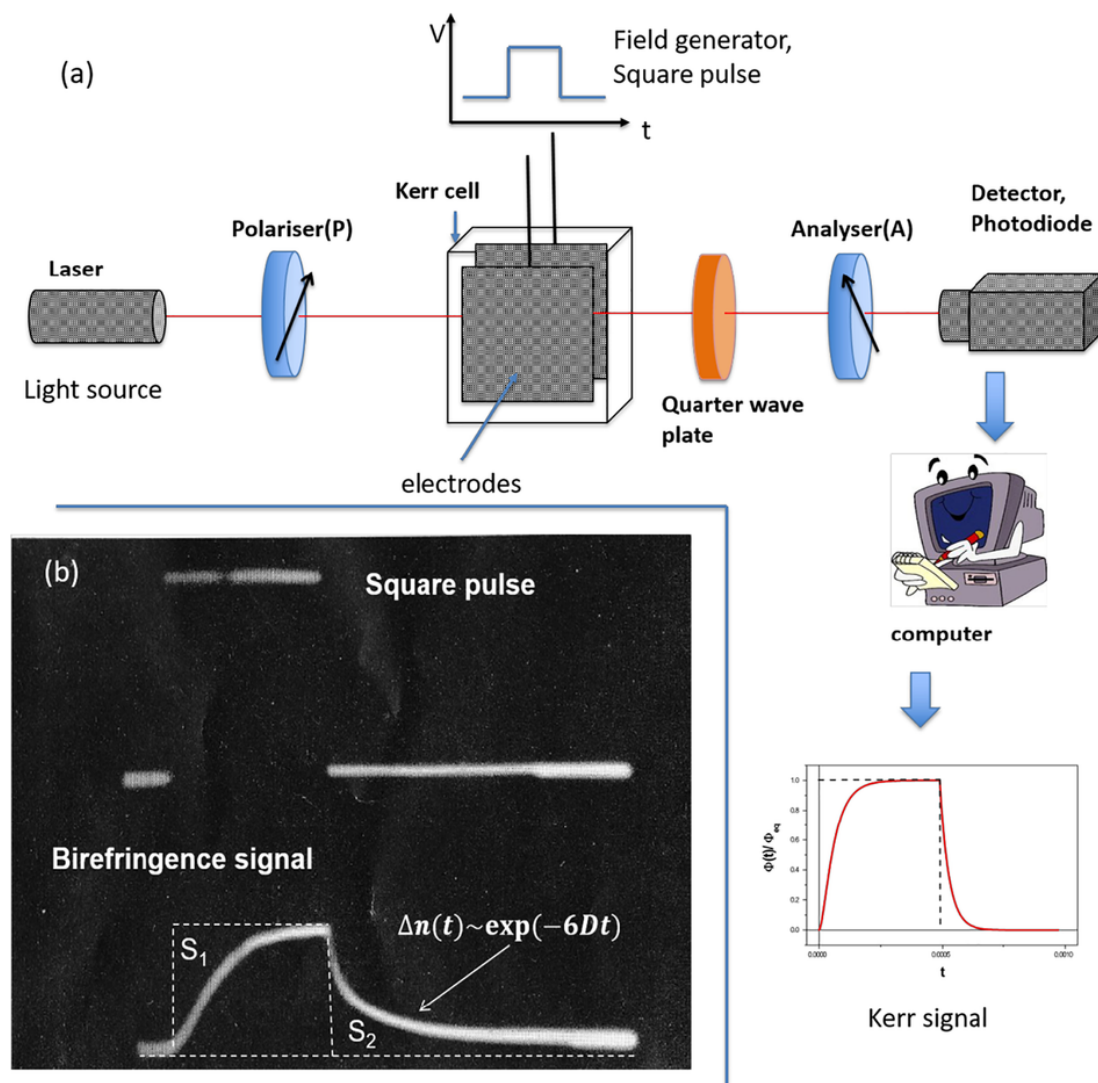


**Fig. 2.** (a) Schematic representation of a typical electro-optic Kerr effect setup. It consists of a light source, for example a laser; a polariser prism placed at  $45^\circ$  with respect to the direction of the applied field; the Kerr cell in which the liquid sample is placed, with two electrodes in order to apply the electric field; the electric field generator that can produce a field in the form of a sinusoidal wave, a pulse or any other; a second polariser (analyser) placed in crossed position with respect to the first polariser and finally the light intensity detector. The quarter wave plate permits the determination of the sign of the birefringence (see cited references in the text for details on the possible setups). (b) Trace of an oscilloscope showing the field applied, a pulse in this case, and the birefringence response. The signal corresponds to a solution of “acide thymonucléique” in water. Figure adapted from Benoit’s thesis [1]. The signal shows the dynamics of orientation of the particles, which go (rise of the birefringence) from being randomly oriented (fig. 1a) to an oriented state (fig. 1b), when the electric field is switched off, the opposite happens (birefringence relaxation).

uid cell was placed between two polarizing Nicol prisms, the first oriented at  $45^\circ$  with respect to the electric field and the second at a crossed position with respect to the first polariser in such a way so that no light passed the second Nicol prism in the absence of an electric field, as explained above (Fig. 2a). Kerr observed that when he applied an electric field across the liquid light from the candle passed through the second Nicol prism, indicating that, in the presence of an electric field, the isotropic liquid behaved as a uniaxial anisotropic system. Among the liquids used in the experiments some had negative and some positive birefringence, which is defined as  $\Delta n = n_{\parallel} - n_{\perp}$ , being  $n_{\parallel}$  and  $n_{\perp}$  the refractive index parallel and perpendicular to the applied electric field respectively (see Fig. 1). He also observed that, in liquids, the birefringence appeared and disappeared almost instantaneously as the field was switched on or off, a result which differed from his previous observations on solids such as glass, quartz and amber resin, for which birefringence appeared and disappeared in periods of time of seconds [4]. Kerr continued working on liquids and improving the experiment, in particular, by introducing a Thomson electrometer, he was

able to measure the electrostatic potentials, making quantitative measurements possible. With this improved setup and after a number of measurements on carbon disulphide [5], he arrived to the conclusion that the birefringence was proportional to the square of the applied electric field intensity,  $\Delta n = n_{\parallel} - n_{\perp} \propto E^2$ . This dependence of the birefringence with  $E$  is known as the Kerr law (see Section 2.1.2) and the proportionality constant as the Kerr constant,  $B$ , so that  $\Delta n = \lambda BE^2$ , being  $\lambda$  the wavelength of the light source. On the physical origin of the electro-optic Kerr effect, Kerr believed that the double refraction induced in the dielectric material was due to some kind of mechanical directional strain, which was produced by the electric stress, in a way similar to that produced on glass directionally stressed by tensions or pressures. Now a day, it is accepted that the effect is not due to any mechanical stress, but is instead a consequence of the orientation of the optically anisotropic particles in the material under the action of the electric field. The orientation is driven by the interaction of the applied field with the permanent and/or induced dipoles of the particles (see Fig. 1). The first to propose this interpretation was Lar-

mor [6] in 1897, some years after Kerr's death. Following Larmor's idea, Langevin [7] was the first to obtain the equations for the Kerr constant in gases, modelled as axil symmetric anisotropic particles without a permanent dipole moment, by setting up the equations for the energy of the molecules as a function of their angle with respect to the electric field, and using the Boltzmann equation in order to obtain the orientation distribution function. The theory of the Kerr constant has been developed since those days [2]. Gans was the first to recognize the existing relation between the value of the Kerr constant and the optical anisotropy of the molecules, and its relation with the degree of depolarization of the scattered light, which was later developed by Debye; a review about the theory of Kerr constant can be found in reference [8] and references therein.

Around the end of the Second World War Benoît started his Ph.D on electro-optic Kerr effect in colloids [1]. In order to be able to study conducting aqueous solutions of DNA, he introduced the pulsed technique [9,10], in which the electric field is applied as short, milliseconds long, square pulses. Benoît noted that the stationary birefringence was not instantaneously generated (see Fig. 2b) and that, once the pulse was over, it took the system a certain time to re-establish the isotropic state, see Fig. 2b. This opened the door to the study of birefringence relaxation. This technique is known today as Transient (time domain) Electric Birefringence, TEB. Benoît developed the theory of birefringence relaxation in his thesis and found that, regardless of the mechanism of orientation; the decay relaxation was proportional to  $\sim \exp(-6Dt)$  being  $D$  the rotary diffusion constant of the colloidal particle (see next sections, Section 2.1.1). The rotational diffusion coefficient can then be related with the size and shape of those particles. O'Konski and Zimm [11] developed a similar device, using short pulses, to study the birefringence relaxation of tobacco mosaic virus (TMV) in aqueous solutions, and arrived to the same relation for the rotational characteristic time,  $\tau = 1/(6D)$ . From their results they were able to estimate the length of the TMV particles. In a subsequent article [12], O'Konski and Haltner performed electric birefringence experiments on TMV solutions applying, in addition to the square pulses used in the previous studies, several types of wave forms: reversing square pulses (see Section 2), exponentially decaying pulses and pulsed sine waves. They found three distinct frequency domain responses of birefringence. The first, occurring around 200 Hz, ascribed to the rotational relaxation of the TMV particle, the second corresponded to a plateau of the Kerr constant extending until 10 kHz, the third region occurred at high frequencies where anomalous dispersion, which had been found to depend on electrolyte concentration, of the Kerr constant was observed. From these results they proposed that the mechanism of orientation of the TMV, which is a charged rod-like particle, is dominated by the counterion polarization along the main axes of the particle, being the contribution of permanent dipole moments, if present, negligible. Other Kerr effect experiments on charged macromolecules followed, and the general conclusion was that counterions play a dominant, but not yet well-understood, role in the orientation mechanism of macroions when subjected to an electric field. The role played by counterions [13–26] in the mechanism of orientation of polyelectrolytes in Kerr effect experiments is central to the understanding of experimental results in polyelectrolyte aqueous solutions and in complex mixtures of polyelectrolytes and surfactants (or any other mixture of surfactants with polymers, proteins, clay or other particles).

On the other hand, the cloud of counterions surrounding charged particles in aqueous solutions seems to play a key role in the observed anomalous orientation of charged colloids when placed in electric fields: under certain conditions, some colloids orientate with their main axes perpendicular to the field, even in the absence of any transversal permanent dipole moment (see Fig. 1), giving place to what is known as *anomalous birefringence signals* [27–32].

Summarizing, the electro-optic Kerr effect gives two kinds of information, one coming from the stationary value of the birefringence, which is related with the particle's size and shape through the anisotropy of the optical and electric polarizability (see Section 2), and the other from the relaxation phenomena involved in the orientation of molecules or colloids. The birefringence relaxation is related with charge distribution, the presence of permanent or induced dipoles and to the particle's size and shapes. Because the decay rate of the birefringence measures the particle rotary relaxation time and, as this parameter is approximately a function of the third power of the greatest dimension of particles [33], it is an extremely sensitive indicator of molecular conformation changes [34] and aggregation processes.

The goal of this review is to highlight the electro-optic Kerr effect as a very useful technique for the study of polymers–surfactants mixtures in aqueous solutions and thus, in what follows, I will give a very short overview of these complex mixed systems, with the sole objective of contextualize the usefulness of Kerr experiments when used to study them. An extensive revision of the state of the art in polymer-surfactant systems is out of the scope of this review, there are plenty of excellent reviews and books on the properties of those systems in bulk and also at interfaces and in films [35–50]. Electric birefringence, even being a bulk technique, can be very valuable for understanding both bulk and surface behaviour, since the former is coupled to the dynamic properties at interfaces, for instance the adsorption/desorption dynamics at fluid and solid interfaces strongly depends on the formation of aggregates in bulk, and so do surface rheology properties at fluid-fluid interfaces [43,45,47–55].

## 1.2. Polymer-surfactant mixtures

Mixtures of polymers and surfactants in aqueous solutions are used in many industrial applications. To name but a few, they are important in the oil and food industries and in the production of cosmetics, detergents, paints and coatings [39,42]. Moreover, mixtures of oppositely charged species can be used as gene carriers in gene therapy, and encapsulation in drug delivery systems [38,39,42,56]. The understanding of the interactions, and of the structures which emerge because of them, in mixtures of polyelectrolytes with opposite charged colloids is of fundamental importance in the study of biological systems as well, for instance in mixtures of DNA and proteins or in the immobilization of enzymes in polyelectrolyte complexes [57]. Life itself is believed to have its origin in molecular self-assembly of increasing complexity and specificity [58] where RNA, a polyelectrolyte, and its interactions with other charged species play a central role as the origin of the first self-replicating systems [59], which eventually gave place to the primitive cell. The features of polymer-surfactant complexes, such as size and shape, have been studied with various techniques including dynamic (DLS) and static (SLS) light scattering, X-ray spectroscopy, and small angle scattering of X-ray and neutrons (SAXS, SANS), among others [50,60–64]. From all these experiments a very complex picture emerges, where a large number of factors are involved. To make things even more complicated, polyelectrolyte-surfactant complexes frequently remain trapped in non-equilibrium metastable states, both in bulk and at interfaces, whose characteristics depend on the history of the systems, for instance on the protocols of mixing or time elapsed before preparation [65–69]. As a consequence, thermodynamic theories ([39]: p.193) cannot be used, in principle, to explain the complex behaviour of these systems

The aggregation of polyelectrolytes and surfactants of opposite charge in aqueous solutions is driven by both electrostatic and hydrophobic interactions, which give place to very rich and complex phase behaviours [35,70,71]. The formation of polyelectrolyte-surfactant aggregates can lead to phase separation, a stable colloidal disper-

sion or soluble complexes, depending on a large number of parameters, such as, charge density of the polyelectrolyte; chain rigidity/flexibility, molecular weight and degree of branching; the charge ratio between polyelectrolyte and surfactants; the kind of polyelectrolyte and surfactant counterions; the hydrophobic/hydrophilic balance of surfactant molecules and chemical groups in the polyelectrolyte chain; the presence of other components, like salt, in the mixture; the physical conditions like pH, temperature, etc. as well as on polymer and surfactant concentrations. Because of the large number of variables which need to be taken into account the search for generalities in the features and behaviour of these systems is a very difficult task, especially when considering that all the variables depend on the specific chemical system under study. The richness and complexity of aggregate structures and properties encountered when dealing with these systems is a consequence of the interplay among all these variables.

Despite the difficulties just mentioned, a general simplified picture of the behaviour of polyelectrolyte-surfactant mixtures in water can be given. As an oppositely charged surfactant is added to a polyelectrolyte aqueous solution, the surfactant ions progressively replace the polyelectrolyte counterions (entropy driven) in the neighbourhood of the polyelectrolyte chain. At low surfactant concentrations, this exchange of counterions does not necessarily lead to effective polymer-surfactant association. This process does not produce, in general, observable changes in the bulk properties of the system, as could be followed with commonly used bulk techniques such as conductivity or light scattering. The changes undergone by the system in this low surfactant concentration region can, however, be detected by the Kerr effect [72,73] because the electric properties, particularly the counterion polarizabil-

ity, around the polyelectrolyte chain changes (see Section 3). As the surfactant concentration increases, the surfactant ions finally condense onto the polymer chain close to charged groups. At a certain specific concentration, which is characteristic of each polyelectrolyte-surfactant system, surfactants begin to cooperatively associate onto the polyelectrolyte chain. By cooperatively we mean that the probability for a surfactant ion to condense onto a binding site on the polymer chain increases if adjacent sites are already occupied. This surfactant concentration is known as the critical aggregation concentration,  $c_{ac}$ . The  $c_{ac}$  occurs at concentrations 1 to 3 orders of magnitude lower than the critical micelle concentration,  $cmc$ , of pure surfactant solutions, and can be determined by calorimetry [74], conductivity and surface tension measurements, among others [48]. The most used method for determining the  $c_{ac}$ , and the amount of surfactant molecules bound to the polyelectrolyte chain, is by potentiometric measurements using surfactant selective electrodes [75–77]. This technique measures the concentration of free surfactant molecules,  $c_f$ , and permits the calculation of the number of surfactants bound to polymer molecules, given by  $c_b = c_s - c_f$ , being  $c_s$  the total surfactant concentration. The results from surfactant selective electrode measurements are generally presented as a plot of the degree of binding,  $\beta$ , as a function of  $c_f$ . This curve is known as the binding isotherm (Fig. 3a). The degree of binding is defined as  $\beta = c_b/c_p$ , where  $c_p$  is the polymer concentration in monomers (in polyelectrolytes is the concentration of charged groups). The binding isotherms have sigmoidal shapes (see Fig. 3) where different zones can be seen and from which the  $c_{ac}$  can be obtained. The features of the binding isotherms depend on the degree of cooperativity in the polymer-surfactant association process, which itself depends on the na-

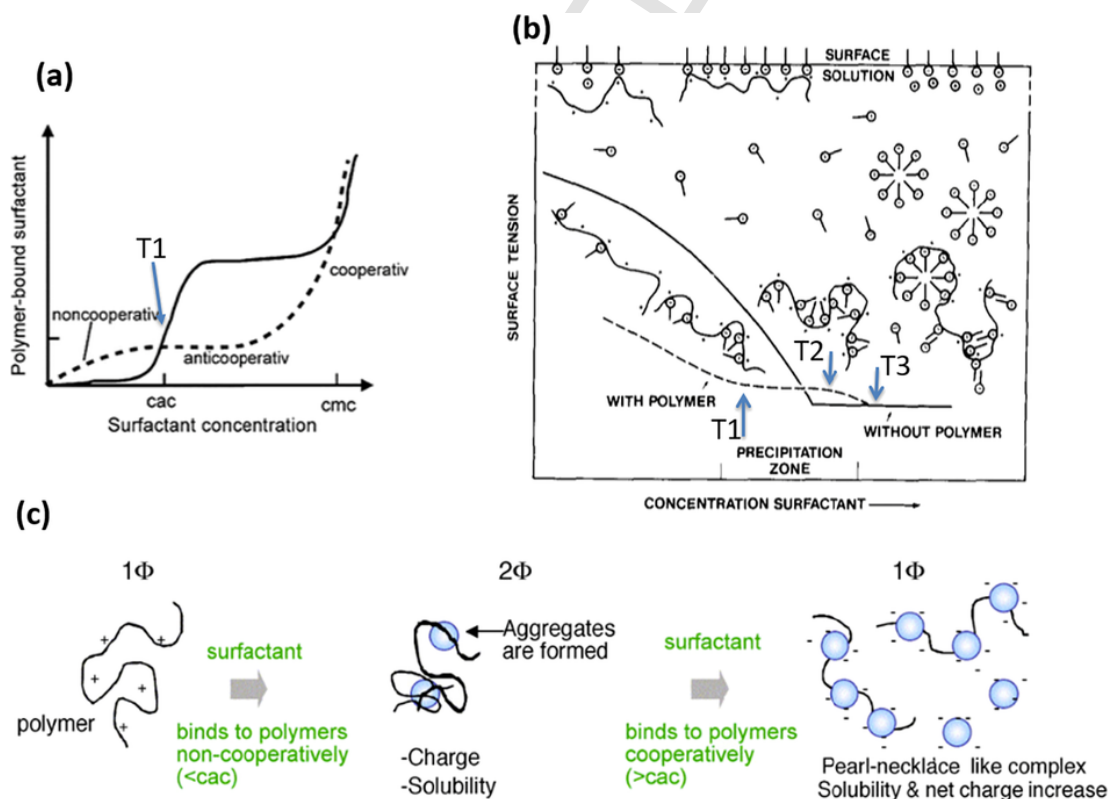


Fig. 3. (a) Schematic binding isotherms for an oppositely charged polyelectrolyte-surfactant mixture. The dotted line represents a binding isotherm where non-cooperative, anti-cooperative and cooperative regions can be observed. The Solid line represents a binding isotherm with a very well defined  $c_{ac}$ . (b) Schematic representation of a surface tension isotherm for polyelectrolyte/surfactant mixtures in water. The solid line represents the surface tension of surfactant solutions without polyelectrolyte, and the dashed line that of the mixture as a function of surfactant concentration. The concentrations T1, T2 and T3 in mixed systems are indicated. (c) Schematic representation of the aggregation process in polyelectrolytes and opposite charged surfactants in aqueous solution. Figures (a) and (c) adapted from [47]: Nylander T, et al., Formation of polyelectrolyte-surfactant complexes on surfaces. *Adv Colloid Interface Sci* 2006;123–126:105–23. Copyright (2006) with permission from Elsevier. Fig. 3b adapted from [78]: Goddard ED., Polymer-surfactant interaction part II. Polymer and surfactant of opposite charge. *Colloids and Surfaces* 1986; 19: 301–29. Copyright (1986) with permission from Elsevier.



ture of the interaction between polymer and surfactant molecules. These interactions can lead to cooperative, non-cooperative (random) or anti-cooperative, surfactant-polymer complexation (see Fig. 3a). Only in the case of cooperative association can a cac be well defined.

As mentioned, the cac can also be determined by surface tension measurements, in that case, the cac is ascribed to the beginning of the first plateau in the surface tension isotherms [78]. Fig. 3b shows a schematic representation of the surface tension isotherm of a polyelectrolyte-surfactant mixture, as a function of surfactant concentration. In this figure, the concentration at which a first plateau appears, labelled as T1, corresponds to the cac. As stated before, at this concentration the surfactant begins to bind cooperatively onto the binding polymer sites. The concentration T2, at which the plateau ends, is generally associated with the saturation of the binding sites on the polymer chain. This concentration corresponds to the beginning of the plateau in the binding isotherm (Fig. 3a). Above this concentration the aggregates become hydrophobic and precipitation may occur. In some systems the precipitates re-dissolve at higher surfactant concentrations [71], in Fig. 3b this occurs at the concentration marked as T3, which are generally higher than the cmc of the surfactant.

The progressive addition of an oppositely charged surfactant to a polyelectrolyte solution results in a partial collapse of the polymer chain, [79] this is due to the partial neutralization of the polyelectrolyte charges, which diminishes the electrostatic contribution to the polymer persistence length. Additionally, there is also a hydrophobic contribution to the polymer collapse due to the addition of surfactants. As stated before, the birefringence relaxation time is very sensitive to the size of colloids in suspension and all these changes can be followed by the Kerr effect with great sensitivity. Often, the formation of multichain complexes are observed as the surfactant concentration increases, the effect on the particle size of aggregation is opposite (size increment) to the effect of chain collapse (size reduction), being this a source of confusion when interpreting the experimental results of, for instance, light scattering on these systems [50]; again, the Kerr effect could be very useful in distinguishing the two processes.

As mentioned before, for some weak polyelectrolytes, the aggregation process is not cooperative at all and no cac can be defined, in those cases the Kerr effect has proven to be a useful and very sensitive technique in the study of the “continuous” aggregation process [73].

With respect to the structure of complexes, Hansson and Almgren [80–83] have shown that surfactant aggregates formed in polyelectrolyte solutions are similar to the micelles formed in pure surfactant solutions, being the main difference that the surfactant aggregation begins at lower concentrations, the cac ( $<$  cmc), induced by the presence of the polyelectrolyte. These results are at the origin of the pearl-necklace model of the complexes [84], see Fig. 3c, which consists of surfactant micelles wrapped (decorated) and interconnected by the polymer chain. However, there are numerous experimental evidences that the complexes formed above the cac can be compact or soft, monodisperse or polydisperse, spherical-like, rod-like or having any other morphology, depending on the features (chemical structure) of the polyelectrolytes and surfactants [50]. In order to gain insight on the influence of polyelectrolyte parameters such as flexibility or degree of charge, computer simulation experiments could be very useful [85]. In this respect let me mention here a very recent work by Goswami et al. [86] in which authors studied by molecular dynamics the effect of the charge density of the polyelectrolyte chain on the structure and dynamics of polyelectrolyte-surfactant complexes. They found that the structures changed from pearl-necklace to nearly spherical shapes with an increase in charge density on the polymer chain. In the context of Kerr effect, I would like to mention here that very little computer simulation has been done on polymers in electric fields [87–90] and none at all, that I am aware of, on polymer-surfactant mixtures, more work on this

subject is very desirable both for electric birefringence experimental analysis and birefringence theory development.

Finally, I would like to stress that the behaviour and properties of polyelectrolyte-surfactant mixtures in aqueous solutions are by far more rich and complex than the simplified picture given above, however, what was said is sufficient to stress the usefulness of electro-optic Kerr effect in the study of these systems in dilute solutions. We will see in Section 2 that the two directly measurable parameters in Kerr effect experiments: the stationary birefringence (or Kerr constant) and the birefringence relaxation times, are both very sensitive to changes in the polyelectrolyte counterion polarizabilities, which are very different if the counterion is a small, such as  $\text{Na}^+$ , or a relatively large surfactant ion. The Kerr constant and birefringence relaxation times are very sensitive to changes in the particle's size and shape as well, which are affected by polymer partial collapse and aggregation that occur when surfactants are added to a polymer solution.

In this review, I will present the basic principles of the electric Kerr effect technique and show the kind of information that can be obtained with it when used to study aqueous solutions of mixtures of polymers and surfactants. In what follows, an overview of the principles and theory of electric Kerr effect is given, Section 2. In Section 3, selected results of electro-optic Kerr effect on mixtures of colloids with surfactants will be presented. The article finishes with the concluding remarks.

## 2. Principles of Kerr effect

Excellent reviews and books [91–97] about the principles, theory, techniques and applications of the electro-optic Kerr effect have existed for many years, here I will give a succinct overview of those principles and theories in their simplest form with the objective of introducing analytical expressions useful for semi-quantitative interpretation of electric birefringence experiments. Thus, the theories that will be described below, and the equations deriving from them, are not intended to be a complete theoretical background on electric birefringence, they are instead those that I found most useful in aiding the interpretation of electro-optic Kerr effect experimental results when applied (carefully) to the study of polyelectrolyte-surfactant mixtures in aqueous solution. Before presenting the theory a few words about experimental realization of electric birefringence measurements are in order. The typical setup was described in the introduction and schematized in Fig. 2, readers can consult the references for details [98,99]. A basic setup for birefringence measurements is relatively easy to put together for demonstrative purposes [100], but obviously, when using birefringence measurements for scientific research, there are experimental details and problems that must be handled carefully. For example, controlling the signal to noise ratio or taking special care when working with conductive solutions [101], or at low temperatures [102], among others. With modern technology, the electronics for fast detection and data acquisition as well as waveform generators and amplifiers, that was a problem some decades ago, are easily accessible today.

In birefringence experiments the electric field can be applied in the form of alternating fields, in which case the technique is known as Frequency domain Electric Birefringence (FEB) [103], or in the form of pulses with different waveforms [12]. When square pulses are used [9–11], the technique is known as Transient (time domain) electric birefringence, TEB.

A very useful version of the pulsed technique, the reversing pulse electric birefringence technique (RPEB) was introduced by O'Konski in 1957 [12]. It consists of first applying a square pulse, (ideally) waiting until the stationary value of the birefringence is reached, and then rapidly reversing the sign of the electric field by applying the same pulse but in the opposite direction (see Fig. 4).

A description of a typical setup for RPEB and its application to solutions of bentonite, a clay, mixed with a cationic surfactant, can be

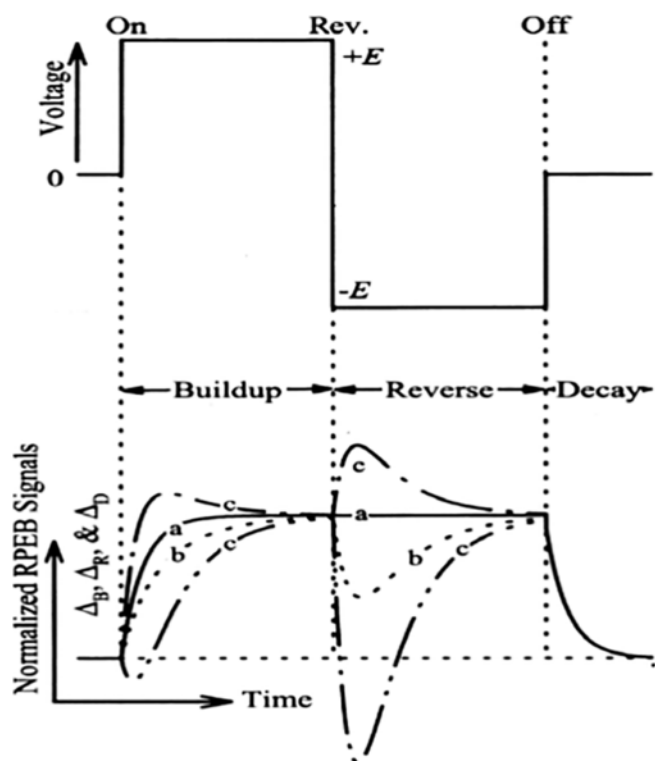


Fig. 4. Schematic representation of the applied reversing-pulse electric field and the corresponding RPEB signals (a-c). (a) Orientation due to the electronically induced dipole moment (no change is observed when the pulse is reversed). (b) Orientation due to permanent dipole moment or ion-fluctuating mean-square-average dipole moment (a "dip" is visible when the pulse is reversed). (c) Orientation due to mixed dipole moments of (dips and humps can be seen in the buildup and reverse processes, respectively). Reprinted from [104]: Yamaoka et al. Theory and experiment of reversing-pulse electric birefringence. The case of bentonite suspensions in the absence and presence of cetylpyridinium chloride. *Colloids and Surfaces A: Physicochemical and Engineering Aspects*, (1999) 148(1–2), 43–59. Copyright (1999) with permission from Elsevier.

found in references [104–106], together with the design of a high voltage bipolar pulse generator in [107].

RPEB is very convenient for determining the contribution of permanent and induced dipoles in the particle orientation mechanism. Because, in general, the induced dipole is established very quickly, compared with the rotational dynamics of the particles, when the sign of the square pulse is reversed, the particle does not have enough time to rotate while the new (opposite in direction) induced dipole is established instantaneously (when compared to rotational motion), thus no change in the birefringence after sign reversal of the external field is observed (curve a in Fig. 4). This behaviour indicates that only fast induced dipoles are responsible for orientation of particles in the field. However, if a change in the birefringence is observed when the sign of the electric field is reversed, then a permanent dipole could be present: due to the presence of the permanent dipole, particles will try to follow the electric field, they rotate in order to align the permanent dipole with the (reversed) field direction which produces a transient change of the birefringence signal (curves b, c in Fig. 4). The behaviour observed is similar to what would happen if a slow induced dipole were present: if the time it takes for the induced dipole to be established is of the order of the rotational relaxation time, it acts as a permanent dipole when the electric field is reversed and the RPEB signals will resemble those obtained if a real permanent dipole were present. The slow induced dipoles can occur in polyelectrolyte solutions when the polarization of the ionic atmosphere is hindered by potential barriers or if the counterions are tightly bonded onto the particle surface, as can happen in mixtures of polymer and charged surfactants.

It is worth mentioning that electric birefringence is not the only electro-optical phenomena observed, the application of an electric field to a colloidal suspension can produce changes in the scattering intensities, fluctuations in the scattered light, dichroism, anisotropy in adsorption and fluorescence. All of these phenomena have their origin in the intrinsic electric and optical anisotropy of molecules and give place to other electro-optical techniques [60,92,93,97]. For instance, a molecule may be able to better absorb light polarised parallel to one molecular axis than another. The application of an orientating electric field produces anisotropy in the absorption of light, this is known as dichroism. Similarly, fluorescence involves absorption of light followed by re-emission at a different wavelength. For fluorescent molecules, the ability to absorb and re-emit light depends on the axis presented to a polarised light beam, the systems fluoresces in a different way if composed by aligned or randomly distributed molecules. The fluorescence method is a very useful electro-optical technique and was used in early studies of DNA, colloids, polymers and liquid crystals [92–94,97].

In the following we will deal with the theory of Kerr effect in liquids but I will restrict myself to the TEB technique.

### 2.1. Theory of birefringence relaxation phenomena

When an electric field is applied to a colloidal suspension, the particles reorient themselves along the direction of the field, this is due to the torque generated by the interaction between the field and the dipoles present [108], or induced [108,109], on the particles (see Fig. 1). This orientation results in a macroscopic anisotropy of the fluid properties, in particular of the refractive indices, as explained in previous sections.

As stated before, in the following I will restrict the discussion to the birefringent transient behaviour in TEB experiments, i.e. the relaxation phenomena resulting from the application of an electric field in the form of square pulses (Fig. 2). The extension of the theory to alternating fields (FEB) and RPEB can be found in references [110–112]. I recall here that, measurement of the time dependent birefringence gives information not only on the anisotropy of dipole moments and polarizabilities, but also of a hydrodynamic quantity, the rotational diffusion coefficient. In rigid colloidal particles, these are determined by their shape and size. As mentioned before, rotational diffusion coefficients depend roughly on the third power of the length of the corresponding axis, therefore measurements of the rotational coefficients are very useful when one wants to detect small modifications in polymer conformation driven by, for instance, the addition of surfactants that bind to their chains.

In what follows we will consider rigid particles containing an axis of symmetry (electrical, optical and hydrodynamics), the case of particles for which both electrical and optical polarizabilities do not have any symmetry was treated by Holcomb and Tinoco [108]. We also assume that the particles are dispersed in very dilute solutions or suspensions, so that interactions between them can be neglected. Under these conditions, the transient birefringence,  $\Delta n(t)$ , generated by the application of an electric field,  $E$ , can be expressed as [113],

$$\Delta n(t) \propto \Delta \alpha^0 \Phi(t) \quad (1)$$

Being  $t$  the time, and  $\Delta \alpha^0$  the intrinsic optical anisotropy of the molecules, the latter is given by  $\Delta \alpha^0 = \alpha_{\parallel}^0 - \alpha_{\perp}^0$ , where  $\alpha_{\parallel}^0$  and  $\alpha_{\perp}^0$  are the optical polarizability, i.e. the polarizability of electrons at the frequency of the laser beam used in TEB experiments (see Fig. 1 and setup, Fig.2), parallel and perpendicular to the main molecular axis, respectively. The orientation factor,  $\Phi(t)$ , gives the degree of orientation of the particles along the field;  $\Phi$  depends on the electric field intensity,  $E$ , the anisotropy of the particle's electric polarizabilities,  $\Delta \alpha^e = \alpha_{\parallel}^e - \alpha_{\perp}^e$  and the presence of a permanent dipole,  $\mu$  on

them (see Fig.1). In the absence of an electric field,  $E = 0$ , the orientation function is zero and the particles are, by thermal agitation, oriented randomly in the fluid, resulting in zero birefringence (isotropic). If the electric field intensity is very high,  $E \rightarrow \infty$ ,  $\Phi \rightarrow 1$ , and the particles are completely oriented in the field direction. In the previous statement it is assumed that the largest electric polarizability and permanent dipole lie both on the symmetry axis of the particle. In the case of particles with permanent dipole moments and for which both electrical and optical polarizabilities do not have any symmetry is very complex and was treated by Holcomb and Tinoco [108].

Now, if  $E$  has a finite value, molecules adopt an equilibrium orientation state, characterized by a stationary-state birefringence ( $t \rightarrow \infty$ ),  $\Delta n_\infty$ , which depends on the field intensity. In a typical TEB experiment we have two transient phenomena, the first begins the moment the field is switched on, and corresponds to the orientation process of the particles, where the birefringence increases until the stationary value,  $\Delta n_\infty$ , is reached (see Fig. 2b). This process is known as buildup relaxation of the birefringence and depends on the mechanism of orientation, i.e. the presence of permanent or induced dipoles. The second process initiates when the electric field is switched off at the end of the pulse, and corresponds to the relaxation of the particles, from the oriented, anisotropic state to their original randomly oriented isotropic state ( $\Delta n = 0$ ). This is known simply as birefringence relaxation and is independent of the orientation mechanism.

The orientation factor is a time dependent function given by [60,112,114,115],

$$\Phi(t) = \frac{\int_0^\pi \frac{3\cos^2\theta-1}{2} f(\theta, t) \sin\theta d\theta}{\int_0^\pi \frac{3\cos^2\theta-1}{2} \sin\theta d\theta} \quad (2)$$

where  $\theta$  is the angle between the particle symmetry axis and the external electric field. Under the assumption of axially symmetric particles in a very dilute non-interacting solution, the function  $f(\theta, t)$ , which represents the probability of finding a particle with its symmetry axis oriented between  $\theta$  and  $\theta + d\theta$ , may be given by the rotational diffusion equation (inertial effects are ignored [114]),

$$\frac{df(\theta, t^*)}{dt} = \frac{1}{\sin\theta} \frac{d}{d\theta} \left( \sin\theta \left[ \frac{df(\theta, t^*)}{d\theta} + \frac{1}{k_B T} \frac{dU}{d\theta}, f, (\theta, t^*) \right] \right) \quad (3)$$

where  $k_B T$  is the thermal energy and  $t^*$  is the reduced time defined by  $t^* = D t$ , being  $D$  the rotational diffusion coefficient about the transverse axis of the particle.  $U$  is the interaction energy of the electric field with the induced and permanent dipole moments of the particle. In the general case,  $U$  is a function of time and the angle,  $\theta$ :

$$U(\theta, t) = -\vec{E}'(t) \cdot \left( \vec{\mu}, +, \underline{\alpha}^e, \bullet, \vec{E}' \right) \quad (4)$$

where  $E'(t)$  is the internal field function [8];  $\vec{\mu}$  and  $\underline{\alpha}^e$  are the permanent dipole vector and the electric polarizability tensor, respectively.

In the simple case where the permanent dipole lies along the symmetry axis of the particle, which is dispersed into a non-conducting media and subject to a small electric field intensity, the field-particle interaction is given by,

$$U = -\mu E'(t) \cos\theta - \frac{1}{2} \left( \alpha_{\parallel}^e, -, \alpha_{\perp}^e \right) E^2(t) \cos^2\theta \quad (5)$$

When the electric field applied is constant, the angular distribution of particles reaches an equilibrium orientation state ( $df/dt = 0$  in Eq. 3). The orientation factor reaches then a stationary value,  $\Phi_\infty$ , which is given by Eq. 25 in Section 2.2, where the subscript “ $\infty$ ” indicates that the stationary orientation state was reached ( $t \rightarrow \infty$ ).

Benoît was the first in solving Eq. 3, for the case of very low field strengths, by expanding  $f(\theta, t)$  in a series of Legendre polynomials to obtain analytical expressions for the birefringence buildup after the sudden application of a uniform homogenous electric field, and for the birefringence relaxation after the sudden annihilation, once the stationary state was reached, of said field. He finally obtained for the buildup transient [10,112,114,116];,

$$\begin{aligned} \frac{\Phi(t)}{\Phi_\infty} &= \frac{\Delta n(t)}{\Delta n_\infty} \\ &= 1 - \frac{3R}{2(R, +, 1)} \exp(-2, Dt) \\ &\quad + \frac{R-2}{2(R, +, 1)} \exp(-6, Dt) \end{aligned} \quad (6)$$

$$\text{With } \beta = \frac{\vec{\mu} \cdot \vec{E}'}{k_B T}; \gamma = \frac{\Delta \alpha^e E'^2}{2k_B T}; R = \frac{\beta^2}{2\gamma} = \frac{\mu^2}{\Delta \alpha^e k_B T}$$

In Fig. 5 we show the relative orientation function,  $\Phi(t)/\Phi_\infty$ , for the buildup relaxation as calculated with Eq. 6 for several values of  $R$ , including negative ones. Note that  $R$  is the ratio of the contribution of permanent to induced dipole moments in the orientation mechanism of molecules and is independent of field strengths. A value  $R = 0$  implies the absence of permanent dipole moments, while  $R \rightarrow \infty$  means that the induced dipole is negligible compared to the permanent dipole contribution. On the other hand, a negative value of  $R$  indicates that the permanent and induced dipoles lie on different axes, so that the permanent dipole has a large component in the direction perpendicular to the main axis of the induced dipole. Note that  $\Phi_\infty$  can be positive or negative and the birefringence sign will be positive or negative depending on the sign of the optical anisotropy (the birefringence sign depends on the product, Eq. 1). Also note that for  $R = -1$  Eq. 6 diverges, this is because the stationary value of the birefringence,  $\Delta n_\infty$ , tends to zero when  $R = -1$  [112].

The buildup birefringence relaxation can be very helpful in the determination of the electrical properties of the particles (molecules, or aggregates), for instance, note that for a pure permanent dipole moment ( $R \rightarrow \infty$ ) the initial slope of the birefringence buildup (see Fig. 5) is zero while for a pure induced dipole it is not ( $R = 0$ ), the buildup relaxation is faster in this last case.

For the birefringence relaxation, when the field is suddenly switched off after the particles reach the stationary orientation state, it was found [10,112,114] that,

$$\frac{\Phi(t)}{\Phi_\infty} = \frac{\Delta n(t)}{\Delta n_\infty} = \exp(-6, Dt) \quad (7)$$

The time evolution of the birefringence is described, under the assumptions mentioned above, by a single exponential with relaxation time  $\tau = 1/(6D)$ . It is from this equation and the measurements of birefringence relaxation times that the rotational diffusion constants can be determined and used to obtain the shape and size of particles (molecules, aggregates) in colloidal suspension (see below in this section).

Note that if only induced dipoles are present,  $R = 0$  and the buildup relaxation, Eq. 6, becomes,

$$\frac{\Phi(t)}{\Phi_\infty} = \frac{\Delta n(t)}{\Delta n_\infty} = 1 - \exp(-6, Dt) \quad (8)$$



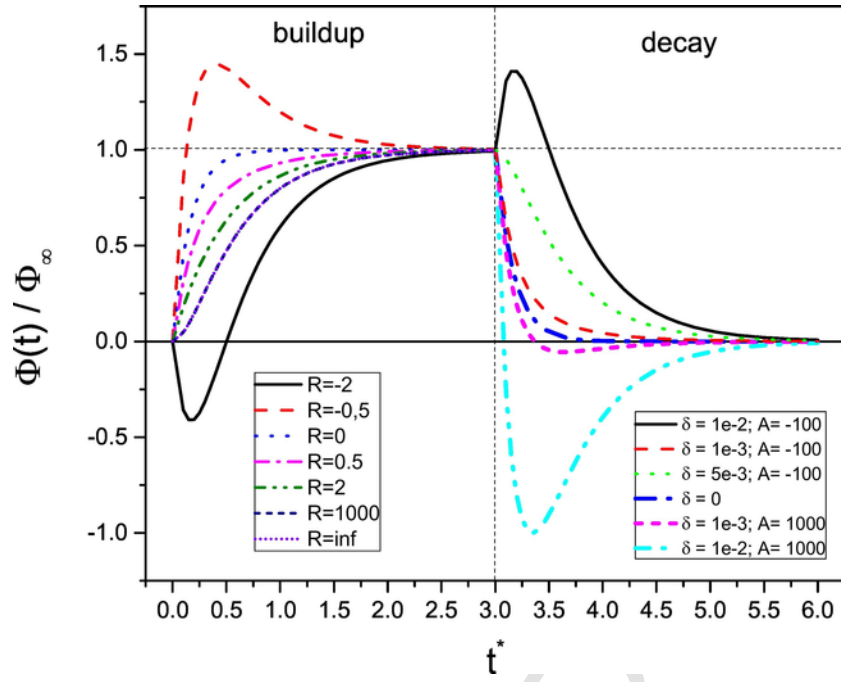


Fig. 5. On the left side of the figure, the relative orientation function as calculated from Eq. 6 for several values of  $R$  is shown. Particles with a pure permanent dipole correspond to  $R \rightarrow \infty$ , and a pure induced dipole to  $R = 0$ . On the right side of the figure the birefringence relaxation is represented in the presence of interparticle interactions, as calculated from Eq. 12. The case with  $\delta = 0$  corresponds to Eq. 7. The electric pulse begins at  $t^* = 0$  and finishes at  $t^* = 3$ . By combining the buildup and decay theoretical curves, the whole TEB signal can be constructed, compare with fig. 2b.

In that case, the buildup and decay relaxations are symmetric curves (Eqs. 7 and 8). Experimentally it could be useful to find the relation between the areas under the buildup curve,  $S_1$ , and below the relaxation curve,  $S_2$ , as indicated on Fig. 2b, this is given by,

$$\frac{S_1}{S_2} = \frac{\int_0^\infty \frac{\Phi(t)}{\Phi_\infty} dt}{\int_0^\infty 1 - \frac{\Phi(t)}{\Phi_\infty} dt} = \frac{8R + 1}{2R + 1} \quad (9)$$

where the last term results from Eqs. 6 and 7. From Eq. 9 and the experimentally measured areas  $S_1$  and  $S_2$ , it is possible to estimate the value of  $R$ . For example, if  $S_1/S_2 = 1$  then  $R = 0$  (Eq. 9) and molecules have no permanent dipole moment, or it is negligible compared with the induced ones. If  $S_1/S_2 = 4$ ,  $R \rightarrow \infty$  and a permanent dipole dominates the orientation mechanism. As stated before, Eqs. 6 to 9 are valid for the limit of very weak fields. O'Konski et al. [117] have calculated expressions for the transient electric birefringence for infinitely strong fields in cases when pure induced or pure permanent dipole moments control the orientation mechanism, Matsumoto et al. [118] obtained an analytical expression for the buildup relaxation for high fields strengths (by including nonlinear terms up to  $E^4$ ) in the presence of both induced and permanent dipoles,

$$\begin{aligned} \frac{\Phi(t)}{\Phi_\infty} &= \frac{\Delta n(t)}{\Delta n_\infty} \\ &= 1 - \frac{X_1}{X_0} \exp(-\lambda_1 Dt) \\ &\quad + \frac{X_2}{X_0} \exp(-\lambda_2 Dt) - \frac{X_3}{X_0} \exp(-\lambda_3 Dt) \end{aligned} \quad (10)$$

where  $X_0, X_1, X_3, \lambda_1, \lambda_2$  and  $\lambda_3$  are all different functions of  $\beta$  and  $\gamma$ ; the expressions for those functions can be found in reference [118]. For very small electric fields, the previous equation reduces to Eq. 6. The analytical expressions of Matsumoto et al. [10] are valid only when  $|\beta^2 + 2\gamma| < 4$ , a general numerical method to solve the equations was presented by Koopmans et al. [119]. An exact treatment of the electro-optic Kerr effect relaxation by Watanabe and Morita can be found in reference [112], this paper contains a brief account of the previous theoretical developments, as was presented above, it also include the analysis and analytical expressions for alternating fields (FEB) and reversed pulses techniques (RPEB).

It is important to remember that the discussion above is based on the assumption of very dilute suspensions of non-interacting particles but, when the concentration is increased, interactions among particles can no longer be neglected, particularly for charged colloids. In the presence of intermolecular pair interactions, expressions for the birefringence buildup and relaxation were obtained [114]. For buildup relaxation it was found,

$$\begin{aligned} \frac{\Phi(t)}{\Phi_\infty} &= 3 \left( \left( 1, -, 2, \frac{\delta}{\beta} \right), +, \frac{1}{2R} \right)^{-1} \left[ \left( 1, \right. \right. \\ &\quad \left. \left. -, 2, \frac{\delta}{\beta} \right), \left( \frac{1 - e^{-6Dt}}{3}, -, \frac{e^{-2Dt} - e^{-6Dt}}{2}, \right. \right. \\ &\quad \left. \left. +, \frac{1}{6R}, (1, -, e^{-6Dt}) \right) \right] \end{aligned} \quad (11)$$

where  $R$  was defined above and  $\delta = u/k_B T$ , being  $u$  the intermolecular pair interaction. This expression is valid for  $\delta < 1$ . Note that Eq. 11 reduces to Eq. 6 when  $\delta = 0$ . For birefringence relaxation in the presence of the same interparticle interactions, the diffusion equation, Eq.

3, can be solved taking  $\beta = \gamma = 0$  ( $E = 0$ ) to yield [114],

$$\frac{\Phi(t)}{\Phi_\infty} = e^{-Dt} \left( 6, -, \frac{\delta^2}{7} \right) - \frac{3\delta}{10} A \left[ e^{-Dt} \left( 2, -, \frac{\delta^2}{5} \right), -, e^{-Dt} \left( 6, -, \frac{\delta^2}{7} \right) \right] \quad (12)$$

this equation is a biexponential function with two relaxation times and reduces to the single exponential decay obtained by Benoît, Eq. 7, in the absence of particle interactions,  $\delta = 0$ . The parameter A depends on R, which can vary between  $\pm\infty$  [114], so that A can be very large, making the second term in Eq. 12 non-negligible even if  $\delta$  is small. Eq. 12, which is represented in Fig. 5 for different values of  $\delta$ , is an oversimplification but I find it useful in helping interpret results from a qualitative point of view.

When strong electric fields are used, birefringence relaxation can depart from monoexponential decays even in the absence of intermolecular/particle interactions due to, for instance, molecular deformation and intramolecular dynamics [120,121].

### 2.1.1. Deformable particles

For flexible macromolecules, the electrical birefringence relaxation is sensitive to the end-to-end distance  $R_{ee}$  of polymer chains, i.e. in their conformation [122] in solution. If we denote by L the extended chain length and by  $l_p$  its persistence length, the end-to-end distance is  $R_{ee} = l_p (L/l_p)^\nu$ , with  $\nu = 2/3$  in good solvent conditions [123]. For flexible chains where  $L > l_p$ , in the dilute regime, it was shown that the birefringence relaxation follows a stretched exponential time variation [124–126]

$$\frac{\Phi(t)}{\Phi_\infty} = \frac{\Delta n(t)}{\Delta n_\infty} \sim \exp\left(-, \frac{t}{\tau}\right)^\beta \quad (13)$$

with  $\beta \sim 1/[1 + 3(1-\nu)]$ ; for  $\nu = 2/3$ ,  $\beta = 0.5$ .

For semiflexible polymer chains ( $L/l_p < 5$ ), Hagerman and Zimm [127] have established, by Monte Carlo analysis, relations between rotational relaxation times and polymer persistence lengths, allowing the estimation of  $l_p$  in the case of moderately flexible wormlike polymer chains [128] by means of electric birefringence experiments even in the absence of a precise knowledge of the local hydrodynamic radius of the molecule. This permits the study of changes in flexibility and/or local polymer conformation as conditions, such as ionic strength or the addition of small surfactant molecules, are varied.

### 2.1.2. Size and shape of particles from birefringence relaxation

In the following we will discuss the relation between the rotational relaxation time and particle size and shape. As discussed above, from the birefringence relaxation time, the diffusion rotational constant D of particles in a dispersant solvent can be calculated ( $D \sim 1/6\tau$ ). The hydrodynamic properties of the molecule in the solvent can be described in terms of frictional coefficients for rotation about three orthogonal axes through the centre of drag. From now on we shall deal with rigid bodies, also considering the absence of any inertial effect. In this case the diffusion constants are related to the friction coefficients by the Einstein relation,  $D_{ii} = \frac{k_B T}{\xi_{ii}}$ , being D and  $\xi$  the rotational diffusion constant and the corresponding frictional coefficient, respectively, “i” is a label for the principal axes of the particles. The analysis of the completely general case, that is, an arbitrarily shaped particle with three different rotary diffusion coefficients, is extremely complicated. We will consider here only the case of molecules with an axis of symmetry

for which two of the rotational constants are equal, say  $D_{11} = D_{22}$  ( $= D$ )  $\ll D_{33}$ , being the last one the diffusion coefficient of rotation about the symmetry axis. Now, the birefringence relaxation time can be expressed in a general form as

$$\tau = \frac{\xi}{6k_B T} \kappa \quad (14)$$

where  $\kappa$  is a dimensionless parameter such that  $0 \leq \kappa \leq 1$ ; for  $\kappa = 0$  we have the full slip condition and for  $\kappa = 1$  the full non-slip or stick condition, this last case is the generally assumed condition for macromolecules in common solvents like water. D ejardin treated the partial slipping conditions in his book [114]. Now, in order to relate the rotational relaxation time to the shape and size of the particles, we need to specify a geometric model for the particles that will permit us to find the friction coefficient. Analytical expressions exist for rigid particles of several shapes [33,87,114,129–131], the case of flexible polymers was also treated using numerical calculations [87,88,132].

In the case of polyelectrolytes a cylindrical symmetry is often assumed; for a rod-like rigid molecule Broersma [131] proposed an expression including end-effect corrections where the rotational relaxation time can be expressed by,

$$\tau = \frac{\pi\eta_0 l^3}{18k_B T} \left[ \ln\left(2, \frac{l}{d}\right), -, 1.57, +, 7, \left( \frac{1}{\ln\left(2, \frac{l}{d}\right)}, -, 0.28 \right) \right]^{-1} \quad (15)$$

where  $\eta_0$  is the viscosity of the solvent,  $l$  and  $d$  are the length and diameter of the rod respectively. Finally, Degiorgio et al. [124,125] showed that the rotational relaxation times measured with electrical birefringence relaxation for a polymer chain with extended length L and persistence length  $l_p$  were consistent with the following expression:

$$\tau(x) = \tau_{rod} \left[ x, +, \frac{(e^{-2x}, -, 1)}{2} \right]^{1.5} \frac{[1, +, 0.54, \ln(1, +, x)]}{x^3} \quad (16)$$

where  $\tau_{rod}$  is the rotational relaxation time of a rod of length L (Eq. 15) and  $x = L/2l_p$ . The last two equations make it possible the study of polymer conformations in solution from birefringence relaxation and how conformation changes when salt or small molecules are added, surfactants for instance, at least from a semi-quantitative approach.

### 2.1.3. Effect of polydispersity in birefringence relaxation

So far, we have not considered the effect of size polydispersity in the birefringence relaxation times, however, perfectly monodisperse systems are hard to find, especially in polymer physics. If the system is polydisperse the birefringence relaxation results of summing contributions of the various species, to obtain [116,117]

$$\frac{\Delta n(t)}{\Delta n_\infty} = \frac{\sum_i \varphi_i \Delta \alpha_i^0 \Phi_{\infty,i}(\beta_i, \gamma_i) \exp(-, 6, D_i, t)}{\sum_i \varphi_i \Delta \alpha_i^0 \Phi_{\infty,i}(\beta_i, \gamma_i)} \quad (17)$$

where  $\varphi_i$  is the volume fraction of component “i” in the pure macromolecular phase and  $D_i$  is the rotational diffusion constant ( $D = D_{11} = D_{22} < D_{33}$ ) for each component. Now, for infinitely high electric fields,  $\Phi_\infty$  will tend to 1 (if the main axes of optical and electric polarizability coincide) and, if the optical polarizability anisotropy is the same for each component, which holds for macromol-

ecules that differ only in length, we obtain from Eq. 17:

$$\frac{\Delta n(t)}{\Delta n_s} = \sum_i \varphi_i \exp\left(-6, D_i, t\right) \quad (18)$$

Thus, the measurement of the birefringence relaxation from the saturated state ( $\Phi_\infty = 1$ , all molecules perfectly oriented in the field) will yield the weight distribution of polydisperse particles simply by analysing the pre-exponential coefficients of all measurable components of the exponential decay curve, Eq. 18.

Finally, an equivalent expression for the buildup relaxation in polydisperse systems can be obtained by replacing the exponential function in the numerator of Eq. 17 by the expression for the buildup orientation function, Eq. 6 [116].

#### 2.1.4. Counterion polarization in polyelectrolyte solutions

We will finish this section with a few words on birefringence in polyelectrolyte solutions. Polyelectrolytes are macromolecules that, when dissolved in water, dissociate into multivalent macroions and small counterions [123]. Current models for polyelectrolyte solutions are generally based on counterion condensation, an idea introduced by Imai and Onishi [133], Oosawa [134] and developed later by Manning. Because of Manning's important contributions, the theory is commonly known as Manning condensation theory [23,135–137]. The basic idea underlying this model is that when the charge density on a linear polyelectrolyte chain exceeds a critical value, such that the electrical potential along the chain reaches the value  $k_B T/e$ , being  $e$  the electron charge, the exceeding charge is neutralized by the counterions. Part of the counterions then condense onto the polymer chain, close to the charged group, so that the chain potential does not exceed  $k_B T/e$ .

These counterions play a very important role in the polarization mechanism [13–25,116,138–142] which occurs when the macromolecules are placed in an electric field, role which is today far from being well understood [13–22,24,25,135,142]. In the presence of an electric field, the cloud of ions that surround the macromolecule chain redistributes over the interface between the molecule and solvent giving place to an induced dipole moment which contributes to the electric polarizability anisotropy,  $\Delta\alpha^e$ , and thus to the orientation factor,  $\Phi(t)$  [116]. It is accepted that the counterion polarization is the dominant contribution (over that of other induced and permanent dipoles) to the orientation mechanism of polyelectrolytes [142]. If only the condensed counterions polarize along the surface of the macromolecule the equations presented above must be modified to take into account the induced dipole due to the deformation of the ion cloud [143–145]. For weak electric fields (Kerr regime) and considering only ion polarization along the particle symmetry axis in the absence of any permanent dipole moment, the buildup relaxation reads [143],

$$\begin{aligned} \frac{\Phi(t)}{\Phi_\infty} &= \frac{\Delta n(t)}{\Delta n_\infty} \\ &= 1 - \left[ 1, \right. \\ &\quad \left. +, \left( \frac{6D\tau_I}{1-4D\tau_I} \right), \left( \frac{q}{q+1} \right) \right] \exp\left(-, 6, Dt\right) \\ &\quad + \left( \frac{6D\tau_I}{1-4D\tau_I} \right) \left( \frac{q}{q+1} \right) \exp\left(-, \left( 2, D, \right. \right. \\ &\quad \left. \left. +, \frac{1}{\tau_I} \right), t\right) \end{aligned} \quad (19)$$

Being  $\tau_I$  the characteristic time of ion polarization along the chain and  $q$  the ratio of the ion polarizability ( $\alpha_i$  which is proportional to the mean square displacement of ions along the chain, see Eq. 32) to the

induced polarizability anisotropy of the molecule (electronic, atomic). The case corresponding to a molecule carrying a permanent dipole along the main molecular axis is treated in reference [144].

When the relaxation time for the diffusion of the ion cloud is comparable to the rotational relaxation time of the whole macromolecule, the birefringence buildup signals given by Eq. 19, are similar to those obtained when a permanent dipole is present [146,147], being this a source of confusion when interpreting birefringence results in polyelectrolyte solutions.

Above only ion polarization along the main particle axis was considered, however, some experiments on polyelectrolyte aqueous solutions evidenced two contributions of opposite sign to the birefringence signals, and ascribed both to the counterion polarization [15–17]. In order to interpret the observations, it was assumed that condensed counterions polarize along the main chain and that free counterions (or loosely bound) polarize perpendicularly, being the contribution to the birefringence signal of each polarization mechanism of opposite sign. This interpretation has not been experimentally proven yet. In this respect, mixtures of polyelectrolytes (or colloidal particles) and ionic surfactants of opposite charge can be used to shed light on the ionic polarization mechanism in polyelectrolyte solutions [28,148] (see Section 3 below). In this case, because the ion cloud can polarize in a direction either parallel or perpendicular to the axis of molecular symmetry, the anisotropy of the ionic polarization must be taken into account and included in the analytical expressions for the buildup relaxation and Kerr constant (see Eq. 33 in Section 3).

The interfacial dipole induced due to the deformation of the cloud of ions, can saturate when strong fields are applied, probably due to the existence of potential barriers for the displacement of the ions on the macromolecular interface [141,149–153]. When this occurs, the induced dipole becomes independent of the electric field intensity.

The problem of the interfacial induced dipoles, the role played by counterions and the mechanism of orientation of charged particles in an electric field is far more complex than the simplified analysis given in the previous paragraphs; a very general discussion with relevant references can be found in references [154,155].

By now, it should be clear to the reader that the problem addressed here is very complex, which makes it difficult to advance in the development of purely theoretical models. This is why computational methods are, in the author's opinion, fundamental to the understanding of electro-optical properties of colloids, particularly in macromolecules [90,156].

#### 2.2. Theory of Kerr constant

In this section we shall deal with the magnitude of the stationary birefringence,  $\Delta n_\infty$ , and the corresponding value of the Kerr constant,  $B$  [8] which is generally defined as,

$$B = \lim_{E \rightarrow 0} \frac{\Delta n_\infty}{\lambda E^2} \quad (20)$$

$B$  is generally expressed in  $\text{m.V}^{-2}$ ; in Eq. 20,  $\lambda$  is the wavelength of the incident light. The Kerr constant is sometimes defined a bit differently [8], for instance it can be defined as a wavelength-independent constant, as  $K = B/\lambda$ , being  $n$  the solution refractive index. When dealing with colloids in suspension, such as polyelectrolytes in water, the magnitude of the measured  $B$  (or  $K$ ) contains contributions of both the solvent and solute,

$$B = B_w \varphi_w + B_p \varphi_p = B_w + \varphi_p (B_p, -, B_w) \quad (21)$$

where  $\varphi$  is the volume fraction and the subscripts “w” and “p” stand for solvent (water) and particle (polymer), respectively. In general, the birefringence of polymers, particularly for biopolymers and polyelec-

trolytes, is large compared to that of water, Eq. 21 reduces then to  $B = \varphi_p B_p$ . The specific “macromolecule” Kerr constant,  $B_{sp}$ , independent of concentration, can be defined as,

$$B_{sp} = \lim_{\varphi_p \rightarrow 0} \frac{B - B_w(1, -, \varphi_p)}{\varphi_p} \approx \frac{B - B_w}{\varphi_p} \quad (22)$$

The theory of Kerr constant is well developed and rigorous for dilute gases and works well for simple liquids and dilute solutions in nonpolar solvents, where molecular interactions are negligible. For macromolecule solutions in polar solvents, such as polyelectrolytes in water, where interactions cannot be completely avoided, the situation is quite different. However, even for such complex systems, the Kerr effect can be very useful to study them in a semi-quantitative or qualitative manner using the existing theories. I shall now introduce these ideas for a simplified model of a very dilute solution of rigid, axially symmetric dipolar molecules. Let me begin with the case of complete orientation of said molecules in the electric field. This implies that we are considering that the field is so strong that all molecules are completely oriented in the direction of the field. Under this condition, the measurement of birefringence is a direct measurement of the intrinsic optical anisotropy of the molecules [117],  $\Delta \alpha^0 = \alpha_{\parallel}^0 - \alpha_{\perp}^0$ . In the previous paragraph we assumed that the main axis of electric polarizability laid on the particle symmetry axis thus, for completely oriented molecules in the electric field, the birefringence is given by [96],

$$\Delta n_s = \frac{2\pi}{9n} (n^2 + 2)^2 N \Delta \alpha^0 \quad (23)$$

being  $\Delta n_s$  the birefringence for very strong fields ( $E \rightarrow \infty$ ), when all the molecules are fully oriented parallel to the field, and  $N$  the number of molecules per unit volume; “s” stands for saturation. If the saturation birefringence can be measured, the intrinsic optical anisotropy can be obtained, and the stationary birefringence for arbitrary field intensities can be expressed as [117],

$$\Delta n_{\infty} = \Phi_{\infty}(\beta, \gamma) \Delta n_s \quad (24)$$

When the electric field applied is finite and constant, the angular distribution of particles reaches an equilibrium orientation state ( $df/dt = 0$  in Eq. 3, Section 2.1), the distribution function is given by the Maxwell-Boltzmann distribution and the orientation factor, Eq. 2, becomes [8,13,92] [93],

$$\Phi_{\infty} = \frac{3 \int_{-1}^1 v^2 \exp(\beta v, +, \gamma, v^2) dv}{2 \int_{-1}^1 \exp(\beta v, +, \gamma, v^2) dv} - \frac{1}{2} \quad (25)$$

where  $v = \cos \theta$ , the subscript “ $\infty$ ” indicates that the stationary orientation state was reached ( $t \rightarrow \infty$ ). Eq. 25 can be solved numerically for any values of  $\beta$  and  $\gamma$ , or used in a fitting procedure of experimental measurements. From Eqs. 23 to 25 the stationary birefringence, which could be used to obtain the Kerr constant by means of definition 20, can be obtained.

For very weak external electric fields and axially symmetric particles, the orientation factor for the stationary state in Eq. 24 has an analytical solution, which reads,

$$\Phi_{\infty} = \frac{\beta^2 + 2\gamma}{15} = \frac{1}{15k_B T} \left( \frac{\mu^2}{k_B T}, +, \Delta, \alpha^e \right) E'^2 \quad (26)$$

This equation is the Kerr law ( $\Delta n \sim E^2$ ). In Fig. 6, the experimentally measured birefringence of an aqueous solution of xanthan, a rigid

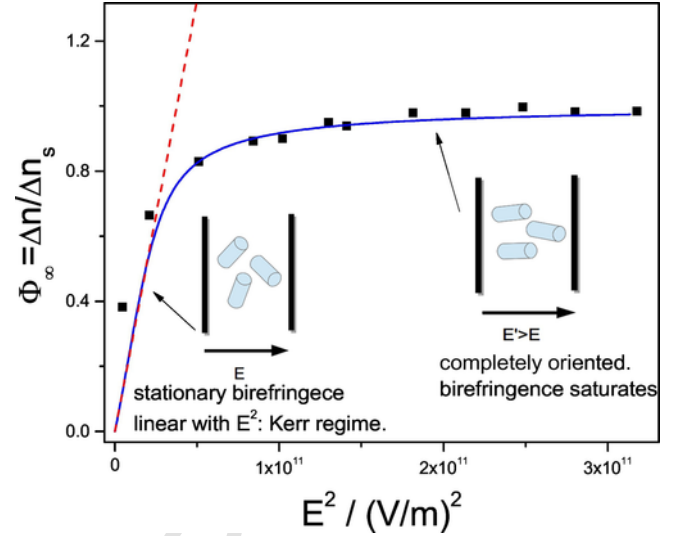


Fig. 6. Electric birefringence measured on xanthan aqueous solutions as a function of field strength (squares). The dashed line corresponds to Eq. 26 and the continuous line to the fitting with Eq. 25. Adapted with permission from Ritacco, H.A et al. *Macromolecules* 2016; 49(15): 5618–29. Copyright 2016 American Chemical Society.

polyelectrolyte, is shown as a function of  $E$  square along with the fitting with Eq. 25 and a comparison with Eq. 26, extracted from reference [28].

As stated before, for polyelectrolytes the induced dipole due to counterion polarization has to be included in the previous equation through  $\Delta \alpha^e$  [143], which has contributions from electronic, atomic and counterions induced dipoles (see Eqs. 32 and 33 in Section 3).

For flexible polymers the theory of the Kerr constant becomes more complex. When an electric field is applied to a solution of flexible macromolecules (or deformable particles) each chemical group or part interacts with the field according to its own electrical properties. Because the groups are linked together, forming the macromolecular chain, they cannot re-orientate themselves freely in the field giving place to a coupled movement of the whole polymer molecule. In this way, all the conformational statistical distribution is affected by the presence of the field. The first model for birefringence in flexible polymers [157] assumed that the polymer chain was formed by a number of ellipsoidal, rigid segments, linked according to a freely jointed chain model. In this case, the birefringence could be calculated by summing the contribution of each segment. If the macromolecule has  $N_s$  segments, each with the same optical,  $(\Delta \alpha^0)_i$ , and electric,  $(\Delta \alpha^e)_i$ , anisotropy polarizability, and with a permanent dipole,  $\mu_i$ , the Kerr constant can be expressed simply as,

$$B = \left\{ \left[ \frac{2\pi}{9n}, (n^2 + 2)^2, N, \Delta, \alpha_i^0 \right], \frac{1}{15k_B T}, \left( \frac{\mu_i^2}{k_B T}, +, \Delta, \alpha_i^e \right) \right\} \frac{N_s}{\lambda} \quad (27)$$

Eq. 27 is obtained under the same assumptions of Eqs. 23 and 26, i.e. rigid, axil symmetric, monodisperse segments. Dows [158] treated the case of a chain formed by ellipsoids linked by freely rotating bonds. A more realistic model, for very dilute polymer solutions and small electric fields, was presented by Nagai and Ishikawa [159]. It consists in averaging the optical anisotropy for all possible orientations of the molecule in the field and over all possible conformations of the polymer chain [160], the final expression can be written as [96],

$$\langle B \rangle = \frac{\pi (n^2 + 2)^2 N}{45 k_B T n \lambda} \left[ \frac{1}{k_B T}, \langle \underline{\mu}^T, \bullet, \underline{\alpha}^0, \bullet, \underline{\mu} \rangle, \right. \\ \left. +, \langle Tr, (\underline{\alpha}^0, \bullet, \underline{\alpha}^e) \rangle \right] \quad (28)$$

where the averages can be obtained with the polymer statistics in the absence of the electric field [161].

Wijmenga and Mandel [162] extended the model of flexible chains to polyelectrolytes assuming a Gaussian chain (theta condition), dilute suspensions, neglecting permanent dipoles and considering only the polarizability of condensed counterions along the main polymer chain for the induced dipoles and in the orientation function. In their model the authors ignore the contribution of non-condensed counterions as well as the interaction among condensed ions. The final expression they obtain for the Kerr constant is,

$$B = \left( \frac{n^2 + 2}{3} \right)^2 \frac{\pi}{n \lambda} \left( \frac{e^2 N_{av}}{27 (k_B T)^2} \right) \left( \frac{(\Delta, \alpha^0)_{mon}}{M_{mon}} \right) l_p^2 f_c z c \quad (29)$$

Being  $(\Delta \alpha^0)_{mon}$  the optical anisotropy per monomer;  $N_{av}$  Avogadro's number;  $e$  the electronic charge,  $z$  the total number of counterions per molecule (or charged groups per molecule),  $M_{mon}$  the monomer molecular mass,  $c$  the polymer concentration;  $l_p$  the persistence length and  $f_c$  the fraction of condensed counterions. This equation shows that  $B$  should increase with polymer concentration, the charge and the fraction of condensed counterions and with the square of the polymer persistence length.

### 3. Electric birefringence in mixtures of colloids and surfactants

In this section results selected from literature will be presented. Unfortunately, there are very few studies on polyelectrolyte-surfactant systems in aqueous solutions which use the Kerr effect as a characterizing technique. This fact led me to write this article in the first place, which I did in hope of stimulating the use of Kerr effect in the study of said systems. The results shown in this section were obtained on polymer-surfactant and particle-surfactant mixtures and they were chosen because of their similarities in behaviour and in order to show how the Kerr effect can help understand both the aggregation process and the role played by counterions in the orientation mechanism of charge colloids in an electric field.

The study carried out by Rudd and Jennings [163] on aqueous solutions of a nonionic polymer, polyvinylpyrrolidone (PVP), mixed with the anionic surfactant, sodium dodecyl sulphate (SDS), was probably the first to use the Kerr effect as a characterizing technique on polymer-surfactant systems. They performed birefringence relaxation and Kerr constant measurements on PVP/SDS solutions at constant polymer concentration and varying the surfactant concentration between 0 and 25 mM. The main result of Rudd and Jennings's paper is the figure reproduced below (Fig. 7). In this figure the Kerr constant,  $B$ , is represented as a function of SDS concentration. Three concentration regions are clearly distinguishable. In region I SDS does not bind to PVP chains; in region II  $B$  increases linearly with SDS concentration, which is explained by the binding of SDS anions to PVP. Due to PVP/SDS complexation the polymer becomes a pseudo polyanion surrounded by  $Na^+$ , the SDS counterions. This cloud of  $Na^+$  ions polarizes the chain in the presence of the electric field, increasing the degree of orientation of the PVP macromolecules and, thus, increasing  $B$  (see the effect of condensed counterions on  $B$  in Eq. 29). They also found that as the SDS concentration increases the buildup and decay birefringence relaxation become more and more symmetric, indicating that the ori-

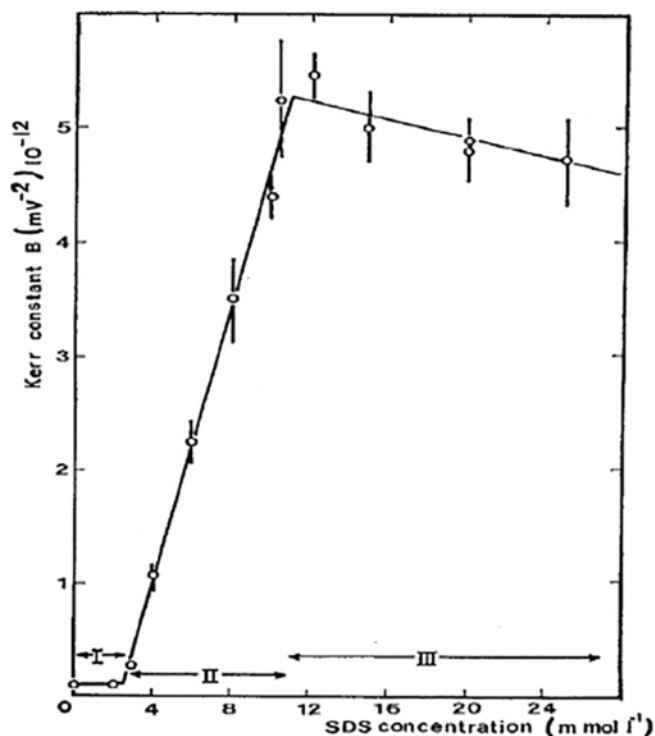


Fig. 7. Kerr constant,  $B$ , as a function of SDS concentration in PVP/SDS aqueous solutions. Three regions are clearly distinguishable reflecting the PVP/SDS aggregation process (see text). Reprinted from [163]: Rudd et al., Electric Birefringence for the Study of Polymer-Surfactant Interactions. The Polyvinylpyrrolidone-Sodium Dodecyl Sulphate System. *Journal of Colloid and Interface Science*, (1974) 48(2), 302-306. Copyright (1974) with permission from Elsevier.

entation mechanism becomes dominated by induced dipoles as SDS bind onto the polymer chain (see Eq. 9 in Section 2). From this result, and considering PVP/SDS complexes as pseudo-polyelectrolytes, they conclude that the main contribution to the orientation function of polyelectrolytes in electric fields comes from counterion polarization, a fact that is accepted today. The existence of the third region, III, is not explained by the authors, however we can now say that the behaviour of  $B$  shown in Fig. 7 is typical of polyelectrolytes in solution. As ionic strength increases,  $B$  diminishes, probably because of partial collapse of polymer chains (see Eq. 29). This supports the idea that PVP behaves as a pseudo polyelectrolyte when mixed with SDS, a fact that is discussed even today [164] but which could have been deduced from the figure below obtained by electric birefringence experiments in 1973.

Rudd and Jennings finish their article by concluding that the electro-optic Kerr effect is a very sensitive and useful technique for studying polymer-surfactant mixtures, even if it is used solely in an empirical manner, and expressing their belief that the method could be very useful for the understanding of the counterion polarization mechanisms in polyelectrolyte solutions, an idea that has inspired recent works [28,148].

In 1975 Wright et al. [165] reported one of the first studies of mixed protein-surfactants systems using electric birefringence as a characterizing technique. They performed experiments on protein-sodium dodecyl sulphate (SDS) complexes using seven different proteins with molecular weights ranging from 11 to 72 kD. In their work they analysed the birefringence relaxation for each system, in order to study the conformation of complexes, and found that the decay curves could be fitted with the sum of two exponential decay processes. They interpreted these results by supposing that the protein-SDS complexes form prolate ellipsoids, and assuming that the slow and fast relaxation times correspond to the rotation of the semi-major axis,  $a$ , about the

semi-minor axis,  $b$ , and the rotation of the semi-minor axis about the semi-major axis, respectively. The slow relaxation, unlike the fast one, was found to depend on the protein molecular weight. From the expression,  $D = \frac{3k_B T}{8\pi\eta a^3} \left[ \ln, \left( \frac{2a}{b} \right), -, 0.5 \right]$  (compare with Eq. 15), for the rotational diffusion coefficient,  $D$ , about the semi-minor axis, they found a relation between the slow birefringence relaxation time,  $\tau_s$ , and the protein molecular weight,  $M$ :

$$\tau_s \propto \frac{M^3}{\ln(M) - 8.4} \quad (30)$$

In Fig. 8 we reproduce their experimental results, which show the validity of the previous equation. The change of slope visible in the plot is explained by assuming a deformable ellipsoidal model, which is compatible with the pearl-necklace model for polymer-surfactants mixtures described in the Introduction (Fig. 3c). This could be the first evidence obtained by the Kerr effect which supports the pearl-necklace model for polymer-surfactant systems. A similar work using TEB for characterizing protein/SDS complexes was published by Rowe et al. [166].

Fairey and Jennings [167] used electric birefringence to study a colloidal dispersion of attapulgita, a rod-like clay mineral, mixed with cetyltrimethyl-ammonium bromide (CTAB), a system which is useful as a model for oppositely charged rigid-polyelectrolyte-surfactant systems. The major objective of their study was to assess the sensitivity of the electro-optic Kerr effect as a technique to evaluate the colloidal stability, particularly in the vicinity of the isoelectric point. The authors used a homemade apparatus to perform dynamic light scattering and electric birefringence measurements simultaneously, which allowed them to measure the translational and rotational diffusion coefficients as well as electrophoretic mobility in the same experimental device. From the saturation of the birefringence at high field strengths (see discus-

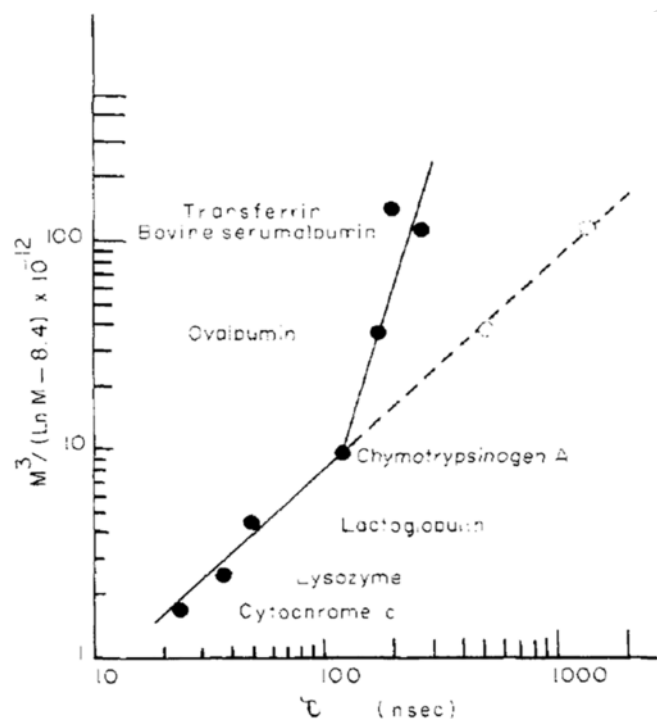


Fig. 8. Protein molecular weight ( $M$ ) as a function of birefringence relaxation times of protein-SDS mixtures. The line corresponds to Eq. 30. The change in the slope might indicate a transition from rigid to flexible particles. Reprinted from [165]: Wright et al. A study of protein-sodium dodecyl sulphate complexes by transient electric birefringence. *Biochemistry*, (1975) 14(14), 3224–3228. Copyright (1975) with permission from Elsevier.

sion in Section 2.2), they were able to obtain the optical polarizability anisotropy of the rod like particles (Section 2.2, Eq. 23) and, from results with ac weak fields, they were able to obtain the electrical polarizability anisotropy of the same particles. From the dependence of the birefringence relaxation time with the strength of the applied field they were also able to deduce the size distribution of the particles in the absence of surfactant by making use of the following expression for the distribution function of the rod lengths,

$$f(l) = \frac{l}{\sigma l(2, \pi)^{1/2}} \exp \left\{ -\frac{1}{2}, \frac{\ln \left( \frac{l}{m} \right)}{\sigma} \right\} \quad (31)$$

where  $\sigma = \left[ \frac{1}{6}, \ln, \left( \frac{D_{R\infty}}{D_{R0}} \right) \right]^{1/2}$  and  $m = \left\{ \frac{3k_B T}{\pi\eta D_{R\infty}}, \left[ \ln, (2, \rho, -, 0.5), \exp, \left( \frac{3\sigma^2}{2} \right) \right] \right\}^{1/3}$ . Here  $D_{R0}$  and  $D_{R\infty}$  are the rotational diffusion coefficients at very low and very high field strengths, respectively, as obtained from birefringence relaxation (see Section 2.1);  $\eta$  is the viscosity of the suspending liquid medium;  $\rho$  is the particle's axial ratio and  $l$  the particle length. All the previous measurements, mobility, rotational and translational diffusion coefficients, as well as the electric anisotropy polarizability ( $\Delta\alpha$ , in Fig. 9) were performed as a function of CTAB concentration, as shown in Fig. 9. The region designated by X in said figure indicates the flocculation zone. Note the large changes on the polarizability anisotropy,  $\Delta\alpha$ , in that region (logarithmic scale) and that the electrophoretic mobility,  $u$ , passes from negative to positive values while  $D_R$  and  $\Delta\alpha$  have a minimum in that region. These results reflect the particle-CTAB aggregation process and are evidence indicating that the rod-like particles are oriented in the field by the counterions polarization. The decrease of  $D_R$  clearly indicates the formation of aggregates before the flocculation zone. These results are quite similar to what is observed in dilute solutions of rigid polyelectrolytes when mixed with oppositely charged surfactants (see results on xanthan-DTAB in reference [28]).

The reversed pulse technique (see Section 2, Fig. 4) was used to study a similar system, an aqueous dispersion of bentonite clay mixed with a cationic surfactant, cetylpyridinium chloride (CPC) [104–106]. In Fig. 10 some of the birefringence signals, obtained for different concentrations of CPC, are reproduced. All signals were obtained at the same field strength. The lines are the calculated signals from a model that considers the polarization of the ion atmosphere along the axis of molecular symmetry [143–145].

Changes in the shape of the signals, and in the sign of the birefringence, can be observed in Fig. 10 as the CPC concentration is increased, these changes are reflected in the values of  $\delta = (27\pi d/\lambda)\Delta n$ , being  $d$  the optical path, which goes from positive to negative as CPC is added. The same happens when the bentonite concentration and field strength are changed (results not reproduced here, see cited reference). These were interpreted by the authors as being a consequence of variations in the relative importance of ion polarization along the chain and induced electronic (and atomic) dipoles. This happens as CPC associates onto the clay particles, or when the concentration of bentonite increases, forming a variety of multiparticle/CPC aggregates that orientate differently in the field giving place to the changes observed. The authors did not consider the role of the polarization of free ions or the possibility of the perpendicular polarization of condensed ions in the orientation mechanism of clay particles. The two opposite effects produced by counterion polarization parallel or perpendicular to the main particle axis could be at the origin of these intriguing anomalous signals [29,31,168]. The behaviour of these systems is similar to that of some mixtures of polyelectrolytes and surfactants of opposite charge, which will be reviewed below (see results on xanthan/DTAB and DNA/



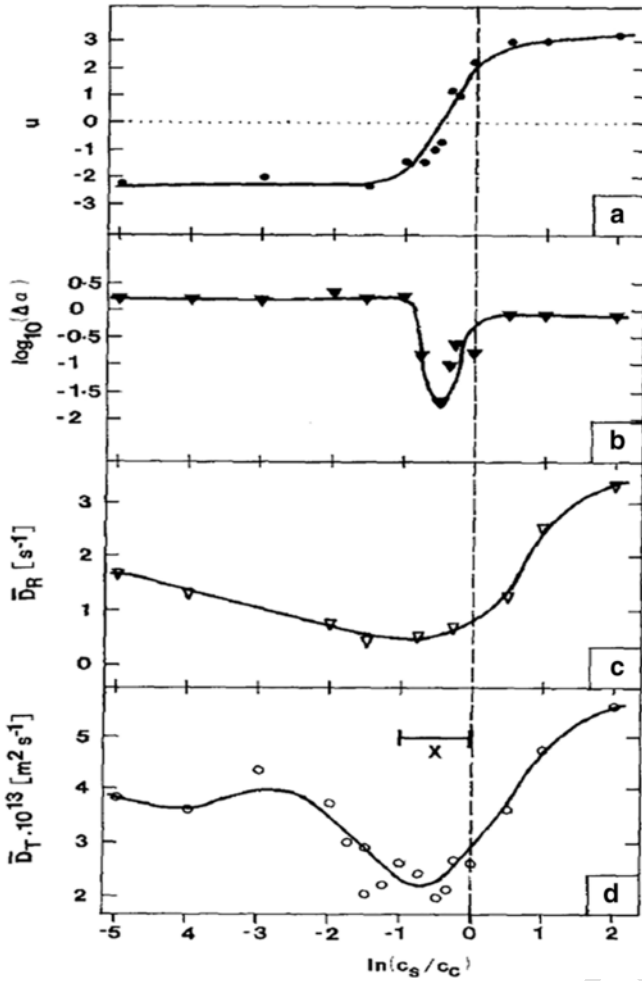


Fig. 9. electrophoretic mobility ( $u$ ), optical anisotropy ( $\Delta\alpha$ ), Rotational ( $D_R$ ) and translational ( $D_T$ ) diffusion coefficients as a function of the concentration ratio  $CTAB(c_s)/attapulgit(c_c)$  in the attapulgit/CTAB mixed systems. Reproduced from [167]: Fairey et al. Electrooptical study of the effect of surfactant on attapulgit clay sol stability. *Journal of Colloid and Interface Science*, (1982) 85(1), 205–215. Copyright (1982) with permission from Elsevier.

DTAB mixtures), where modifications in the fraction of loosely bond and condensed counterions could be at the origin of the changes observed in the shape and sign of their TEB signals.

Cavasino et al. [169], used the Kerr effect and other techniques to study the interactions of polyacrylic and polymethacrylic acids aqueous solutions mixed with a zwitterionic surfactant, tetradecyldimethylaminoxide [169]. From the measurement of the Kerr constant and birefringence relaxation times they conclude that the surfactant produces a progressive conformational transition of the polyelectrolyte chain. They found that the birefringence changes from positive to negative values at a certain surfactant concentration, a behaviour that, as was mentioned, is observed in other polyelectrolyte-surfactant systems [28,148]. They also observed that the Kerr constant passes through a maximum at a surfactant concentration just below the isoelectric point of the polyelectrolyte, this is consistent with the maximum commonly observed in the sizes of polyelectrolyte-surfactant complexes at a certain surfactant concentration as measured by light scattering. This can be interpreted as the result of two opposite tendencies, a growth in size due to aggregation and the opposite effect due to partial collapse of polymer chains.

Foweraker et al. [170] and Isles et al. [171] conducted birefringence relaxation experiments on mixtures of proteoglycan and

hyaluronic acid (see Fig. 11). Cartilage proteoglycans consist of a protein backbone about 400 nm long, with approximately 100 sidechains, each about 40 nm in length. The proteoglycans are found in cartilage, mainly as large aggregates involving hyaluronic acid. The authors were capable of following the proteoglycan-hyaluronic acid aggregation by Kerr effect and found, as in the previous examples, a change in the sign of the birefringence (see Fig. 11b and d) at a certain concentration of added hyaluronic acid. They were able to obtain, from the birefringence relaxation times, the size and aspect ratio (assuming an ellipsoidal particle) of these aggregates in close agreement with results from other techniques. The change in the sign of birefringence indicates a reversal of the optical (or electrical) anisotropy from the proteoglycans to the aggregates as hyaluronic acid molecules bind to the protein core.

The same authors studied, using the Kerr effect, free hyaluronic acid proteoglycan aqueous solutions at very high electric fields [172] and they found very complex buildup birefringence signals, where three contributions to the total birefringence, being some positive and some negative, are clearly observed at strong enough electric fields. This behaviour could be caused by deformation of the particles due to the high field strength, but it could also have its origin in the dynamics of counterion polarization as was proposed for other similar systems (see below).

Our group has studied the interactions between a flexible polyelectrolyte, with variable degree of charge, and an opposite charged surfactant [148]. The systems were a mixture of a cationic surfactant with an anionic statistical co-polymer made of neutral acrylamide monomers and charged acrylamido methyl propane sulfonate monomers (PAMPS). PAMPS with different ratios,  $f$ , of the number of sulfonated monomers to the total number of monomers were used. They were named P50, P25, P20 and P10 corresponding to  $f = 0.5, 0.25, 0.2$  and  $0.1$ , respectively. The cationic surfactant used was dodecyl trimethyl ammonium bromide (DTAB). For P20 and P25 we found that the birefringence was negative in the absence of DTAB, but became positive as the DTAB concentration was increased (see inset Fig. 12b), as happened in the systems described previously in this section (Fig. 11). This behaviour is not observed when salt is used instead of DTAB, in that case the birefringence tends to zero, but does not change sign. In Fig. 12a we reproduce these results for P20-DTAB mixtures. In order to interpret the data, we used a simple empirical model in which we consider the polarization of free and condensed counterions as the only responsible for the orientation mechanism of particles in the field (see Fig. 12b). We assumed that free (or loosely bound) counterions polarised perpendicularly to the main polymer axis, while condensed ones did so parallel to said axis, giving place to contributions of opposite sign to the total birefringence. We estimated the anisotropy of electric polarizabilities,  $\Delta\alpha^e = \alpha_{\parallel}^e - \alpha_{\perp}^e$ , by assuming that ion polarizabilities were of the order of the mean-square diffusion length, the end-to-end distance  $R_{ee}$  for  $\alpha_{\parallel}^e$  and the correlation length  $\xi$  for  $\alpha_{\perp}^e$  (see Fig. 12b),

$$\alpha_{\perp}^e = \frac{\langle \mu_{\perp}^2 \rangle}{k_B T} = \frac{e^2 \xi^2}{k_B T}; \quad \alpha_{\parallel}^e = \frac{\langle \mu_{\parallel}^2 \rangle}{k_B T} = \frac{e^2 R_{ee}^2}{k_B T} \quad (32)$$

With this, the Kerr constant reads,

$$B \sim c \frac{\Delta\alpha^0}{15 k_B T} \left\{ \frac{(1, -, \varphi) f e^2 R_{ee}^2}{k_B T}, -, \frac{\varphi f e^2 \xi^2}{k_B T} \right\} \quad (33)$$

where  $e$  is the electron charge,  $f$  is the nominal charge per monomer,  $c$  the polymer concentration (in monomers) and  $\varphi$  is the fraction of free counter-ions ( $f_c = (1-\varphi)$ , is the fraction of condensed counterions). Note that Eq. 33 results from Eq. 27 neglecting any permanent dipole

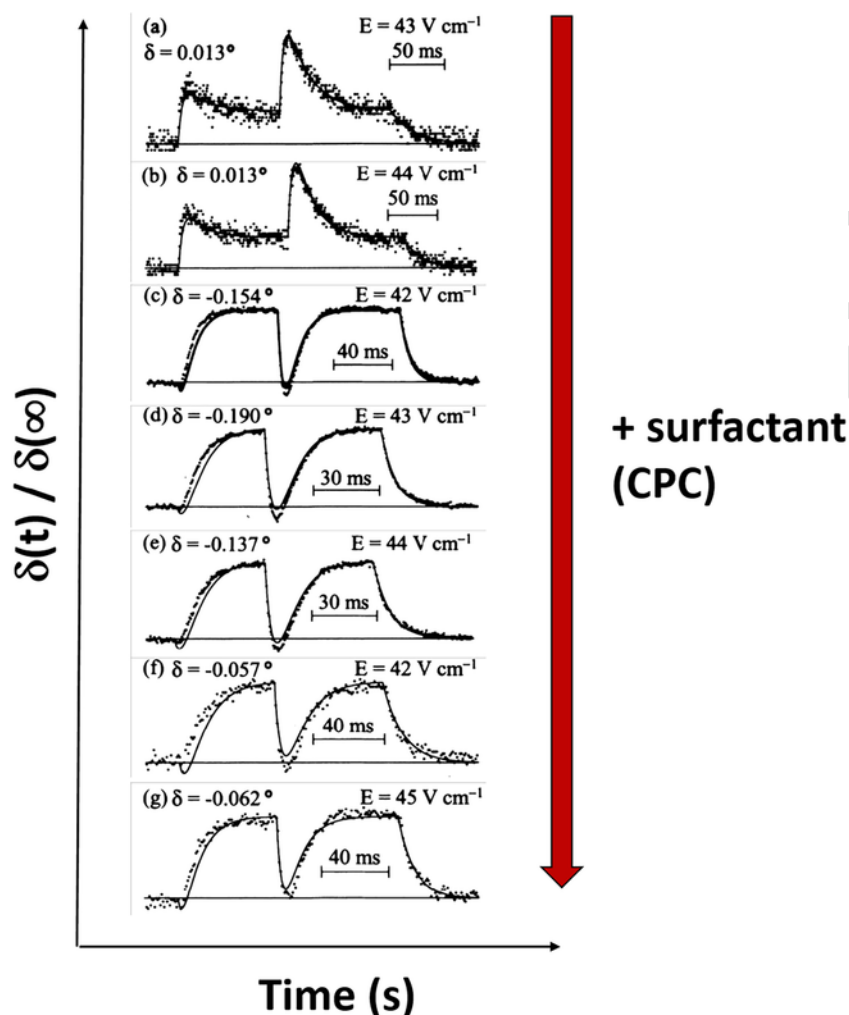


**Fig. 10.** Observed and calculated RPEB signals of bentonite and CPC/bentonite systems, for weak electric fields. Concentrations of CPC (mM): (a) 0, (b) 0.001, (c) 0.05, (d) 0.1, (e) 0.5, (f) 0.9, (g) 1.3. Concentration of bentonite (g/l): 0.005. Note that the sign of the birefringence is indicated by the value of the optical retardation,  $\delta = (27\pi d/\lambda)\Delta n$ , and that it changes sign as CPC is added. Solid lines are theoretical curves calculated using a theory based on counterion polarization. Adapted from [103]: Yamaoka et al. Theory and experiment of reversing-pulse electric birefringence. The case of bentonite suspensions in the absence and presence of cetylpyridinium chloride. *Colloids and Surfaces A: Physicochemical and Engineering Aspects*, (1999) 148(1–2), 43–59. Copyright (1999) with permission from Elsevier.

and calculating the electric polarizability anisotropy with Eqs. 32, note also the similarities with Eq. 29.

Making use of scaling arguments for the polyelectrolyte chain we were able to obtain an analytical expression to fit the data and explain the behaviour observed when salt and surfactant were added: the addition of an oppositely charged surfactant changes the fraction of condensed counterions,  $(1-\phi)$ , producing the change in the sign of B from negative to positive as indicated by Eq. 33.

Returning to Fig. 12, note that B changes sign at the isoelectric point EP (EP is defined as the point for which the concentration of  $\text{DTA}^+$  ions that equals the concentration of the polyelectrolyte  $\text{Na}^+$  original counterions). At the EP concentration, which is about 0.4 mM, the behaviour of PAMPS-DTAB mixtures begins to differ from salt-polymer solutions (B does not change sign as NaBr is added). The cac of P20-DTAB, as measured by surface tension, is indicated in the figure, and coincides with the maximum of B, which occurs at around 1 mM. Note that three surfactant concentration regions can be delimited in Fig. 12, one below the EP, the second between EP and the cac and the third for  $c_{\text{DTAB}} > \text{cac}$ , which is similar to what was found for PVP/SDS (Fig. 7). This behaviour can be rationalized as follows: up to the EP concentration, B diminishes as DTAB concentration increases due to the partial collapse of the polyelectrolyte chains, as happens with salt.

At the EP concentration some DTAB ions condense onto the polymer chain non-cooperatively, B changes sign and increases because the fraction of condensed counterions increases continuously as DTAB is added, Eq. 33, until the cac is reached. At the cac, and driven probably by hydrophobic interactions, DTAB associate cooperatively to the previous aggregates. At concentrations higher than the cac, multichain aggregates could form increasing their sizes, but making them less anisotropic from the optical point of view (see Fig. 1c), reducing  $\Delta\alpha^0$  and thus B. At surfactant concentrations over 4 mM precipitates can be seen, supporting the idea of large multichain aggregates forming at concentrations above the cac. The results of birefringence relaxation (unpublished results) also support the interpretation outlined above. For P10-DTAB mixtures the birefringence does not change sign as DTAB is added, in that case the association process is not cooperatively at all and no cac can be clearly defined by means of surface tension, as is commonly found in weakly charged polyelectrolytes [73,148]. For P10-DTAB mixtures, B increases continuously until it reaches a constant value at a DTAB concentration of about 0.8 mM, which seems to indicate a continuous aggregation process until it saturates [73]. Birefringence relaxation, on the contrary, passes through a maximum as DTAB concentration is increased, this also happens at 0.8 mM in DTAB. This result seems to indicate a starting point for a conformational tran-

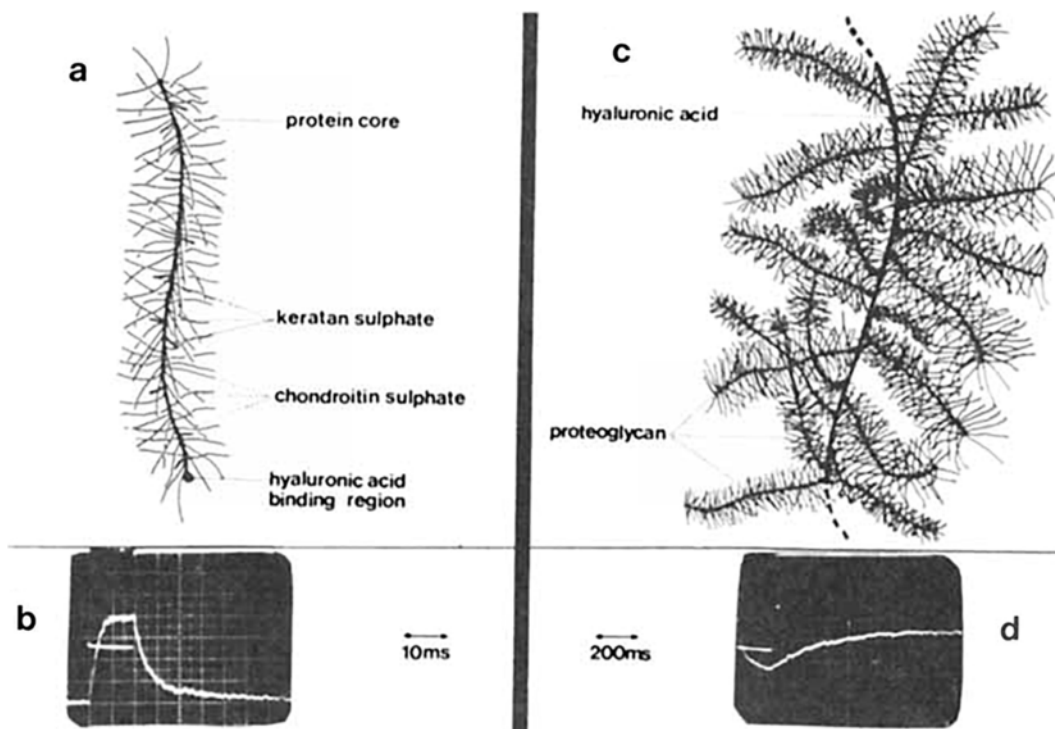


Fig. 11. Proteoglycan and its aggregation with hyaluronic acid. (a) and (c) are schematic diagrams of the structure of a proteoglycan molecule and of the aggregate, respectively. (b) and (d) are the transient electric birefringence signals for each system. In both cases the applied field was of  $360 \text{ V cm}^{-1}$ . Reprinted from [168]: Foweraker et al. Electric birefringence studies of cartilage proteoglycan aggregation. Biopolymers, (1977). 16(6), 1367–1369. Copyright (1977) with permission from John Wiley and Sons.

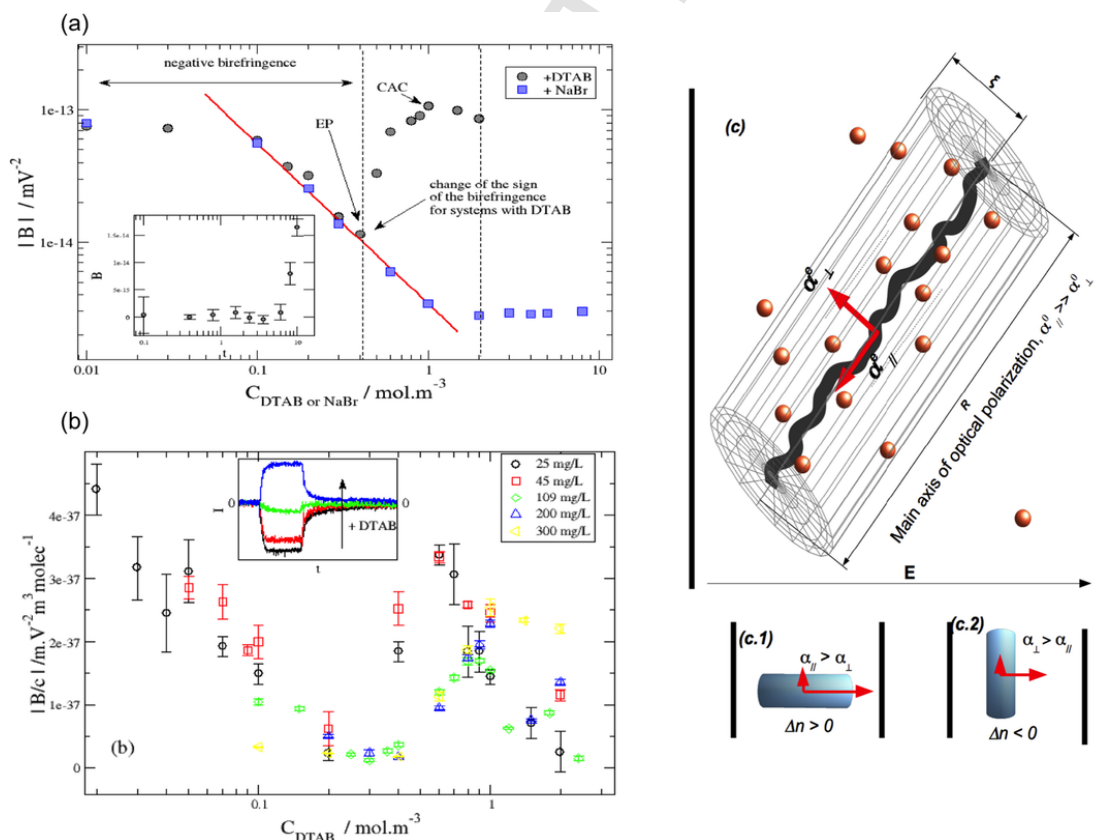


Fig. 12. (a) Modulus of the Kerr constant,  $B$  as a function of surfactant (DTAB) and salt (NaBr) concentration in a P20 solution ( $109 \text{ mg L}^{-1}$ ). (b) The same as in (a) but for P25, and for different polymer concentrations. The inset in panel (b) shows the birefringence signals going from negative to positive as DTAB concentration increases. (c) Representation of the model used for interpreting the data. Adapted with permission from Ritacco HA et al. Macromolecules 2009; 42: 5843–50. Copyright 2009 American Chemical Society.

sition at that surfactant concentration, giving place to more compact, hydrophobic aggregates [73].

A similar study was carried out in a mixture of a rigid polyelectrolyte, xanthan, and an oppositely charged surfactant, DTAB, in aqueous solution [28]. In those systems it was found that, depending on the surfactant and polymer concentrations and on the strength of applied electric field, a negative contribution to the stationary birefringence appears. Recall that a negative birefringence contribution indicates a tendency to orientate the particle (polymer chain, aggregate, etc.) with its main optical axis (which can differ from the main, geometrical particle axis, e.g. DNA) perpendicular to the electric field (Fig. 1d), this is what it was mentioned in the introduction as anomalous birefringence. In Fig. 13 we show a series of electric birefringence signals obtained at several electric fields intensities. Note that the anomalous, negative contribution during the buildup process increases and its relaxation time becomes shorter as  $E$  increases.

These anomalous birefringence signals are not found at low polymer ( $< 60$  ppm) concentrations, whatever the surfactant concentration or field intensity. The anomalous behaviour appears only if the polymer concentrations is larger than  $100 \text{ mg.L}^{-1}$  and when the surfactant is present. This was interpreted as follows: above the cac, the surfactant ions are bound to the polymer backbone, being able to leave the polymer chain only when aggregates of parallel rods are formed, see Fig. 13e. This perpendicular polarization produces a torque that tends to orient the chains with their main axes perpendicular to the applied electric field. This leads to two different polarization mechanisms, one tending to orientate the particles parallel and the other perpendicular to the field, giving place to a positive and a negative contribution to the birefringence (see scheme in Fig. 13e). The negative contribution is especially important at surfactant concentrations above the cac and at high field strengths. All the results obtained in reference [28] are consistent with Manning's theory [31] which ascribes the anomalous signals to the perpendicular polarization of condensed counterions when aggregates of parallel rods with aggregate cross sections of size comparable to the polymer chain length, are formed. These results are also compatible with the ideas expressed by Hoffmann et al. [29] about the origin of anomalous birefringence signals in several colloidal systems.

The xanthan/DTAB system is an example of a colloid, for which birefringence saturation can be reached relatively easily. In Fig. 14a the relative birefringence is represented as a function of  $E^2$  for different DTAB concentrations. The lines are fittings with Eq. 25 from which the values of the electric anisotropy polarizability were estimated and rep-

resented on Fig. 14b as a function of DTAB concentration. The cac in these systems is about  $0.3 \text{ mM}$ , just above the maximum value of the anisotropy in the electric polarizability showed in Fig. 14b.

The electric birefringence relaxation times in xanthan/DTAB mixtures are quite complex. The relaxation dynamic is not well described by monoexponentials, there are at least three relaxation times involved, one ascribable to the rotational diffusion of the aggregates. The origin of the other two is not clear. They could be due internal relaxations modes, particle polydispersity, conformational dynamics of the polyelectrolytes or even due to the existence of interparticle interactions as those considered in Section 2.1. The buildup relaxation is complex as well, but with only two relaxation times. In Fig. 15 a birefringence signal corresponding to a mixture of xanthan and DTAB, obtained at a very high electric field pulse, is shown.

As a last example on the use of electric Kerr effect as a tool in the study of polymer-surfactant systems, some results for DNA-DTAB mixtures in water will be presented. DNA solutions were one of the first systems to be studied by modern Kerr effect [1] and one of the polyelectrolytes more commonly characterized by electro-optic measurements since [120,128,150,153,173-179] (see also chapters 10 and 11, and references therein, in [60]). Dilute aqueous solutions of DNA exhibit a strong negative stationary electric birefringence. I will first explain the origin of this large negative birefringence. In order to result in a negative value of  $\Delta n$ , the optical anisotropy ( $\Delta\alpha^0$ ) and the orientation factor ( $\Phi_\infty$ ), in Eq. 26, must have opposite signs so that the main optical polarizability axis orientates perpendicular to the field (see Fig. 1d). Because of the symmetry in the double helical DNA structure, the occurrence of a significant permanent dipole moment seems unlikely, thus the main mechanism involved in the orientation of molecules in the electric field has to be attributed to induced dipoles which, in the case of DNA, are mainly due to the polarization of condensed counterions along the chains [180]. Thus, the main axis of DNA has to be oriented parallel to the electric field. This means that  $\Delta\alpha^0$  for DNA should be negative if it is to have a negative birefringence. In general, the electrons responsible for optical polarizabilities are the  $\pi$ -electrons, Takashima [181] ascribe the negative birefringence of DNA to the fact that the stacking of bases on the DNA structure is such that their planes lie along the transverse DNA axis, thus, no  $\pi$ -electron polarizability is possible along the major helix axis, resulting in a negative optical polarizability ( $\alpha_\perp^0 > \alpha_\parallel^0$ ). Now let us see what happens when an oppositely charged surfactant is added to DNA solutions.

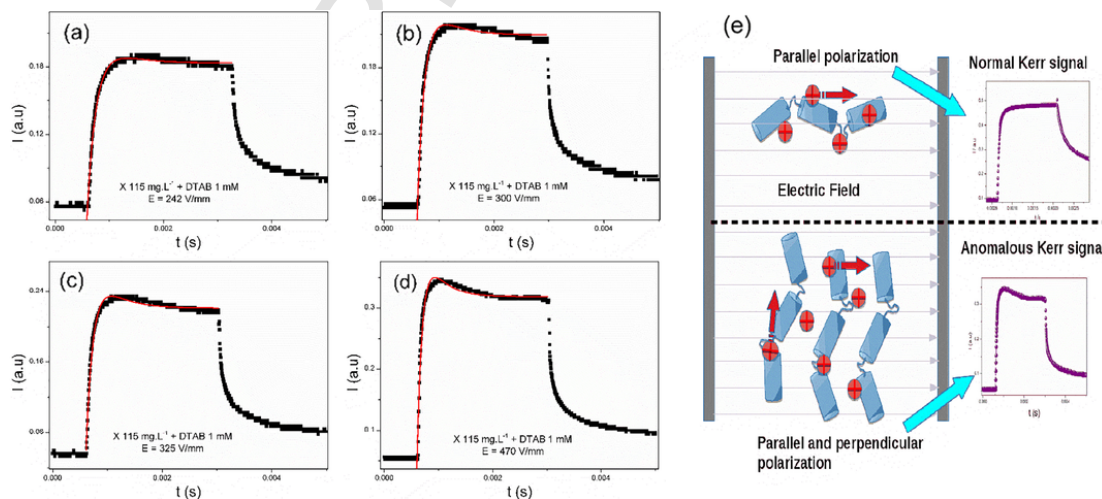


**Fig. 13.** Electric birefringence signals for xanthan (115 ppm)/DTAB (1 mM) aqueous solutions for different field intensities: (a)  $E = 242 \text{ V/mm}$ ; (b)  $300 \text{ V/mm}$ ; (c)  $325 \text{ V/mm}$ ; (d)  $479 \text{ V/mm}$ . (e) Illustration representing a possible interpretation of the data (see text). Adapted with permission from Ritacco, H.A et al. *Macromolecules* 2016; 49(15): 5618–29. Copyright 2016 American Chemical Society.



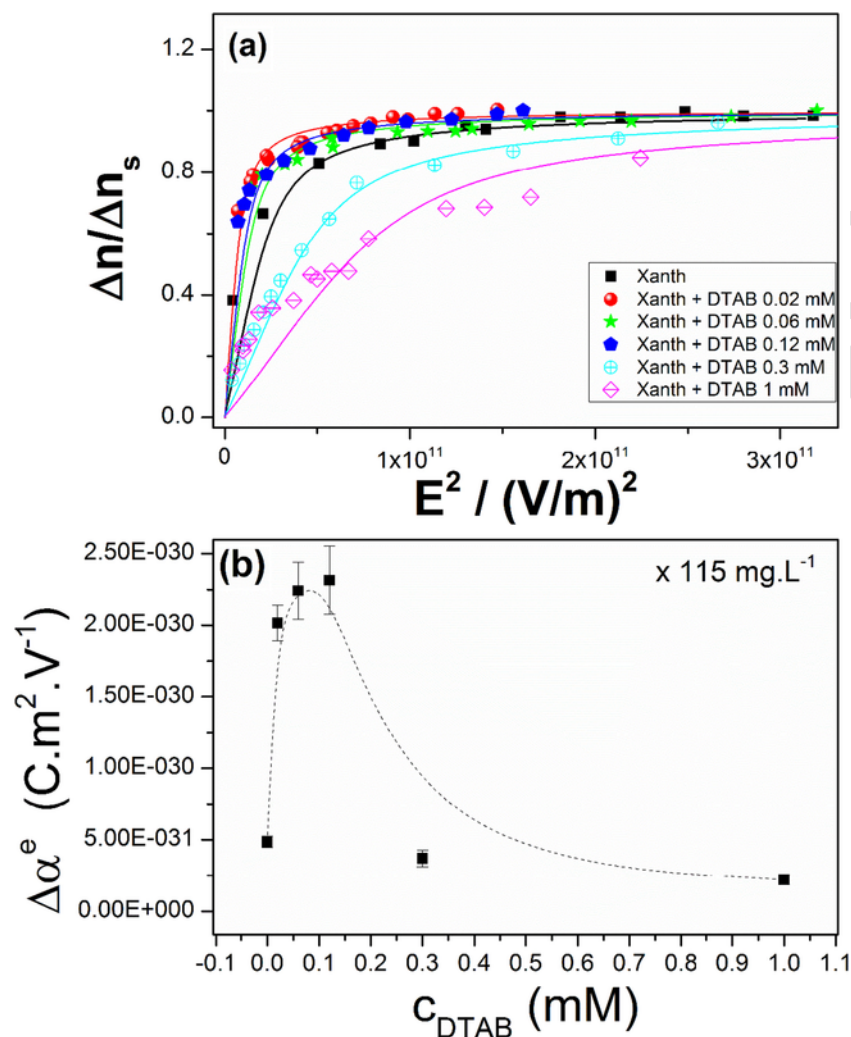


Fig. 14. (a) Relative birefringence as a function of  $E^2$  for several xanthan ( $115 \text{ mg L}^{-1}$ )/DTAB mixtures in water. (b) Anisotropy of the electric polarizability as obtained by fitting the curves in (a) with Eq. 25. Adapted with permission from Ritacco, H.A et al. *Macromolecules* 2016; 49(15): 5618–29. Copyright 2016 American Chemical Society.

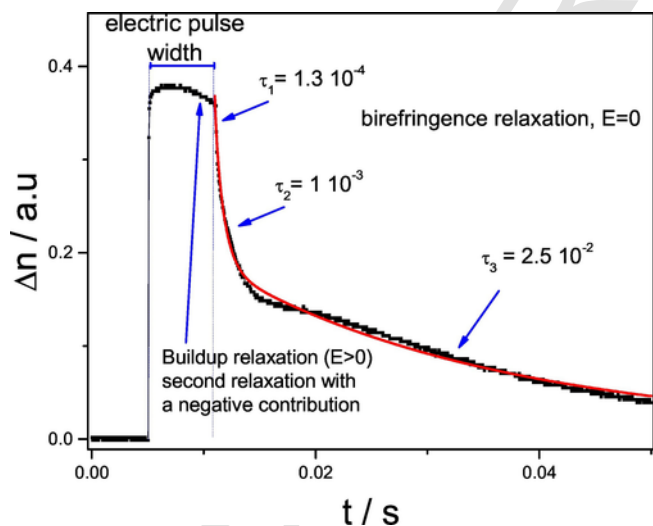
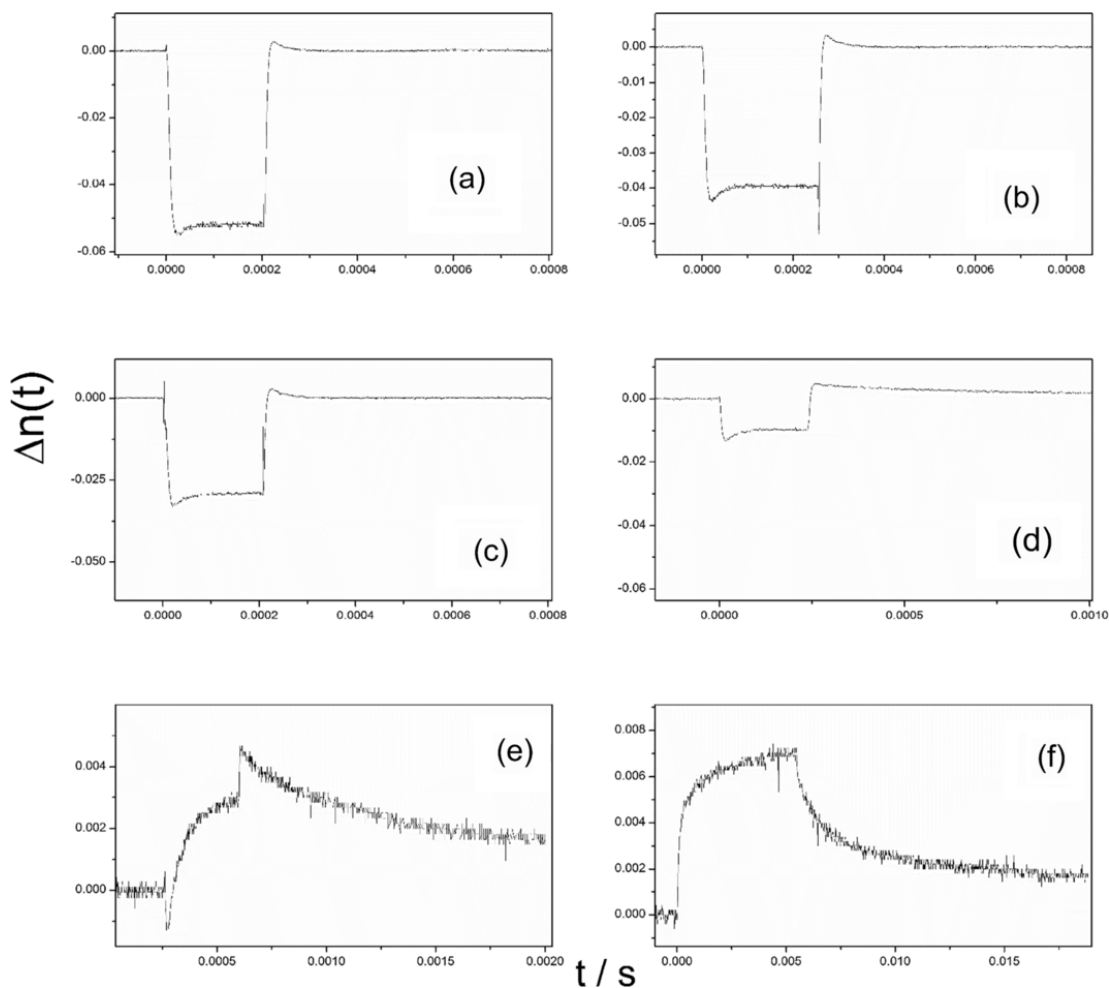


Fig. 15. Anomalous Birefringence signal for a mixture of xanthan 115 ppm and DTAB 0.02 mM, in water. The electric pulse applied was 750 V/mm. Anomalous relaxation phenomena are clearly seen in both built-up and decay birefringence relaxation. Adapted with permission from Ritacco, H.A et al. *Macromolecules* 2016; 49(15): 5618–29. Copyright 2016 American Chemical Society.

For the experiments we used short DNA fragments which were prepared by sonication of Calf thymus DNA (Sigma-Aldrich), the final molecular weight distribution was checked by electrophoresis and  $M_w$  was 300 base pairs, with a polydispersity of 1.2. All experiments were carried out with a DNA concentration of  $360 \text{ mg.L}^{-1}$  and in the presence of salt (2 mM in NaBr). Solutions were prepared by mixing equal volumes of the DNA and surfactant, both at twice their final concentrations. Transient Electric Birefringence experiments were carried out in a homemade apparatus described elsewhere [28]. In Fig. 16a a TEB signal of a DNA solution is shown, we note first that the stationary birefringence is negative and second, there is a positive contribution to the buildup curve with a slow relaxation time (note the similarity with the signals on xanthan solutions, Fig.13). The appearance of these anomalies in the birefringence signals depend on field strength, pulse width, DNA and salt concentration [120,179,182]. Hoffmann et al. published a review [29] about anomalous Kerr signals and show that these anomalies occur in systems as diverse as micellar solutions, polyelectrolytes and clays, viruses and fibres dispersions. In all these systems the anomalous signals are present at concentrations when the colloidal particle lengths, including the thickness of the electric double layer, are about the same as the mean distance between them. Under these circumstances counterions (of the charged colloid involved) could be able to polarize perpendicular to the main particle axis passing from one colloidal particle to an adjacent producing a torque that



**Fig. 16.** Birefringence signals for DNA/DTAB solutions obtained at similar electric field strengths. DNA concentration of  $360 \text{ mg L}^{-1}$  in  $2 \text{ mM}$  solution of NaBr. DTAB concentrations are (a) 0; (b)  $0.2 \text{ mM}$ ; (c)  $0.6 \text{ mM}$ ; (d)  $1 \text{ mM}$ ; (e)  $1.3 \text{ mM}$ ; (f)  $2 \text{ mM}$ .

orientate the set of particles (not necessary an aggregate) perpendicular to the electric field, this idea is similar to the theory proposed by Manning to explain the anomalous birefringence signals observed in certain charged colloidal systems [31] and to what we used above to explain the behaviour of xanthan/DTAB solutions, see Fig. 13c. Because it implies a collective motion, this second process would be slow compared with the normal orientation of chains in the direction of the field. This would explain why the contribution of opposite sign to the birefringence appears only after a certain time, as can be seen in the anomalous Kerr signals of Fig. 16. The maximum observed in the birefringence signals during the buildup process could be then a consequence of these two opposite orientation tendencies. The fact that the anomalous signals depend on the pulse width in TEB experiments [120] can be explained as well: the anomaly in the Kerr signal is seen only if the pulse width is longer than the second relaxation time. Because counterions play a central role in the mechanism just described, a change in behaviour is expected if the original counterions are exchanged by surfactant ions. Figs. 16b to 16f show a series of electric birefringence signals on DNA/DTAB mixtures in aqueous solutions (unpublished results).

Note that as the DTAB concentration increases, from Fig. 16a to Fig. 16f, the stationary birefringence becomes less and less negative, but both positive and negative contributions to the buildup relaxation remain (they are anomalous), furthermore, the positive contribution to the stationary birefringence seems to be independent of the DTAB concentration. At a DTAB concentration of  $2 \text{ mM}$ , the negative contribu-

tion disappears, Fig. 16f. For DNA-DTAB mixtures in  $20 \text{ mM}$  salt a cac of about  $1.3 \text{ mM}$  was determined from binding isotherms [183], this is close to the point where the stationary value of the birefringence changes from negative to positive (see Fig. 16d to 16e). We are compelled to conclude that the association of DTAB ions onto the DNA chains at the cac is responsible for the change in sign of the birefringence. Speculating about the reasons of this behaviour one could think that, as DTAB ions aggregate onto DNA molecules, they remain fixed to the chains by electrostatic and hydrophobic interactions, reducing their mobility; they cannot polarize easily along the chains, thus, the induced dipole becomes smaller reducing the absolute value of the birefringence. For concentrations above the cac, DTAB promotes the formation of multichain aggregates which has the effect of reducing the optical anisotropy, making the birefringence positive and the relaxation times larger (see Figure 16e and 16f). This interpretation is supported by the fact that at DTAB concentrations over  $2.5 \text{ mM}$  precipitates appear in the solutions.

It is also known that the presence of anomalies on the Kerr signals of DNA solutions depend on the electric field strength applied. In Fig. 17 we show the stationary birefringence as a function of  $E^2$  for DNA solutions (Fig. 17a), and for the same solution but with  $1 \text{ mM}$  of DTAB (Fig. 17b). Note that for DNA solutions, the birefringence follows the Kerr law (it increases, in absolute values, linearly with  $E^2$ ) until a critical value of the electric field,  $E_c$ , is reached. Then, the modulus of the birefringence begins to diminish linearly until  $\Delta n_0$  reaches a positive value at high enough electric field intensities. This behaviour can be



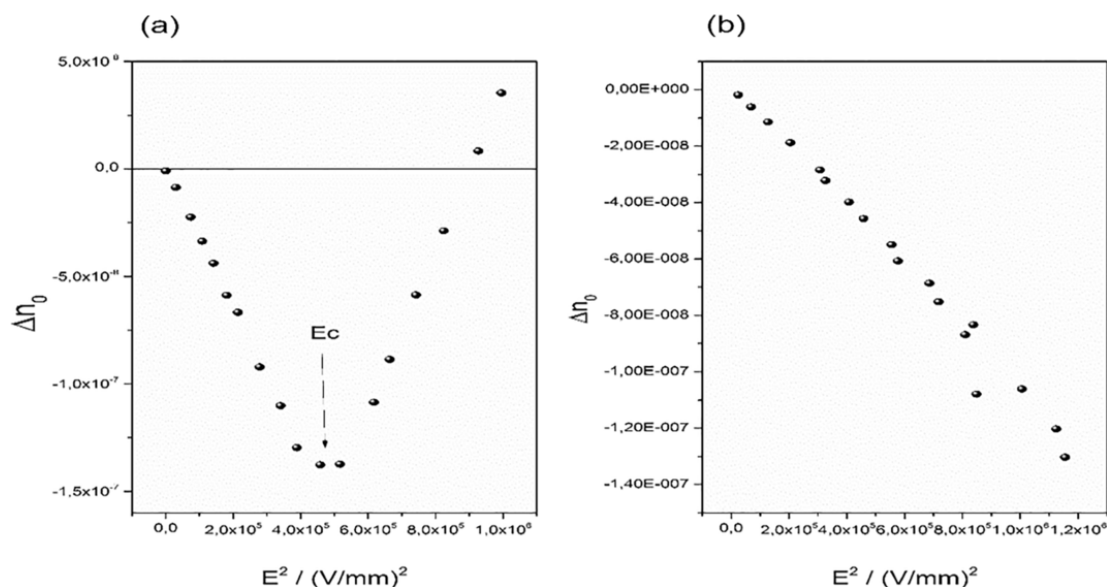


Fig. 17. Stationary birefringence as a function of  $E^2$ . (a) DNA 360  $mg\ L^{-1}$  in 2 mM NaBr aqueous solutions; (b) same as (a) with 1 mM DTAB.

rationalized as follows; below  $E_c$  the negative contribution driven by the polarization of condensed counterions along the chain dominates, and the birefringence increases following the Kerr law. At  $E_c$  the counterion polarization along the main chain axis saturates [141,149–153] and remains constant. At fields over  $E_c$ , the positive contribution, which is probably due to the perpendicular polarization of counterions, begins to play an important role. This contribution increases linearly with  $E^2$  apparently following the Kerr law, but because the constant negative contribution is always present ( $E > E_c$ ), the absolute value of the total birefringence diminishes continuously, eventually reaching a positive value. Why the positive contribution appears only when  $E > E_c$  could be explained by proposing that, a counterion polarization perpendicular to the main polymer axis arises when the energy barrier, which prevents them from leaving the macromolecule onto which they are condensed, can be overcome.

For the system with DTAB at a concentration of 1 mM, the birefringence roughly follows the Kerr law, without changing sign, at least in the range of fields explored. In this case the DTAB ions are strongly associated to the DNA chain by electrostatic and hydrophobic interactions, as indicated by the binding isotherms [183], complicating their polarization in both parallel and perpendicular directions. As a consequence, the saturation of the negative contribution to the birefringence is not seen and the critical  $E_c$  is not reached, at least at the electric field intensities used. The interpretation given above on DNA-DTAB mixtures is only tentative and preliminary, a complete analysis of stationary and birefringence relaxations results is currently in progress and the results will be the object of a future article. It is worth mentioning that the samples are not affected by the application of the strong fields; for each sample all measurements were carried out from low to high fields ( $E > E_c$ ) and then in the opposite direction being the curve perfectly reproduced in both directions indicating that no permanent structural changes in DNA samples took place.

#### 4. Concluding remarks

The Electro-optic Kerr effect is a very sensitive and useful technique for characterizing the optical anisotropy and shape of molecules, particles and colloids in solution or suspension. Because of its sensitivity to small changes in the electric environment of particles in suspension, the electric Kerr effect is a unique tool to study the association processes in mixtures of oppositely charged species, particularly in

polyelectrolyte-surfactant systems. The strong dependence of the rotational diffusion constant with the particle size ( $\sim L^3$ ) makes electro-optic birefringence a remarkably powerful technique in the characterization of polymer-surfactant aggregates. Although birefringence signals contain very rich and unique information about the systems under investigation, the results obtained from birefringence experiments (TEB, FEB and RPEB) are frequently interpreted just qualitatively. The main difficulty in the interpretation of birefringence data on charged colloids is the absence of a well-established theory. The origin of this is, of course, the complexity of the problem, but also the absence of systematic experimentation in well controlled systems in order to evaluate the effect of the variables/parameters involved. These days, with the capabilities of chemical synthesis and the power of calculus with modern computers, a combination of systematic birefringence and numerical experiments on well controlled systems is needed in order to understand the role played by each relevant parameter. The synthesis of new polyelectrolytes with designed features such as rigidly/flexibility and degree of charge; as well as colloidal particles of different and well controlled shapes (spheres, ellipses, cylinders, etc.) and surface charge density, would be desirable in order to formulate specifically designed colloidal systems for Kerr effect experiments. Birefringence experiments in such systems could be of fundamental importance in order to gain physical insight allowing the improvement of theories and permitting the analysis of birefringence results on a more quantitative basis. This is the spirit of a very interesting paper published by Mantegazza et al. [30] on mixtures of rod-like and spherical particles and also of our work on mixtures of flexible and rigid polyelectrolytes with surfactants of opposite charge [28,148].

Despite the complexity of theoretical analysis and other difficulties, electric Kerr effect has proved to be a valuable experimental technique in the study of polymer-surfactant complexation as, I hope, was demonstrated in this article. Electro-optic Kerr effect is of course not restricted to the systems treated here, it can, and has proved to be, a useful experimental technique in the study and characterization of systems such as surfactant solutions, micelles, vesicles, viruses, polymers, nano and microparticles in suspension, membranes, bacterial cells and many more [94]. A recent and very interesting application of Kerr effect is in the study of polyelectrolyte multilayers built onto anisotropic (non-spherical) colloids. These are examples of self-assembly of opposite charged species and thus a good candidate to be studied by the electric Kerr effect. Radeva et al. [184–189] have used the method to

study a series of systems obtained by the Layer-by-Layer (LbL) technique, they have used electro-optic Kerr effect in order to obtain information on structure and electrical polarizabilities including the determination of multilayer thickness, the release of counterions when adsorbing onto the colloids and the calculation of the number of chains adsorbed.

I hope this review will stimulate more experimental and theoretical work on electric Kerr effect as a tool in the study of oppositely charged colloids.

## Acknowledgments

I thank the editor, Francisco Monroy, for inviting me to contribute to this issue in honor of who was one of my PhD advisors and model in science, Dominique Langevin. Support from Agencia Nacional de Promoción Científica y Tecnológica (ANPCyT, Argentina) under grant PICT 2013 (D) no 2070; and Consejo Nacional de Investigaciones Científicas y Técnicas (CONICET, Argentina) under grant PIP GI no 11220130100668CO, is gratefully acknowledged. This work was partially supported by grants PGI-UNS 24/F067 and PGI-MayDS 24/MA09 of Universidad Nacional del Sur (Argentina).

## References

- [1] H. Benoît, Sur un dispositif de mesure de l'effet Kerr par impulsions électriques isolées, Université Louis Pasteur, Strasbourg, France, 1949.
- [2] C.T. O'Konski, A History of Molecular Electro-Optics. Mol. Electro-Optics, Springer US, Boston, MA, 1981–25, [http://dx.doi.org/10.1007/978-1-4684-3914-4\\_1](http://dx.doi.org/10.1007/978-1-4684-3914-4_1).
- [3] J. Kerr, LIV, A new relation between electricity and light: dielectric media birefringent (second paper), Philos Mag Ser 4 (50) (1875) 446–458, <http://dx.doi.org/10.1080/14786447508641319>.
- [4] J. Kerr, A new relation between electricity and light: Dielectric media birefringent, Philos Mag Ser 4 (50) (1875) 337–348, <http://dx.doi.org/10.1080/14786447508641319>.
- [5] J. Kerr, XXII. Measurements and law in electro-optics, Philos Mag Ser 5 (9) (1880) 157–174, <http://dx.doi.org/10.1080/14786448008626821>.
- [6] J. Larmor, A dynamical theory of the electric and luminiferous medium. Part III. Relations with material media, Philos Trans R Soc A Math Phys Eng Sci 190 (1897) 205–493, <http://dx.doi.org/10.1098/rsta.1897.0020>.
- [7] P. Langevin, Sur les biréfringences électrique et magnétique, Le Radium 7 (1910) 249–260, <http://dx.doi.org/10.1051/radium:0191000709024900>.
- [8] C.T. O'Konski, Theory of the Kerr Constant. Mol. Electro-Optics, Springer US, Boston, MA, 1981–119–146, [http://dx.doi.org/10.1007/978-1-4684-3914-4\\_6](http://dx.doi.org/10.1007/978-1-4684-3914-4_6).
- [9] H. Benoît, Sur un dispositif de mesure de l'effet Kerr par impulsions électriques isolées, Comptes Rendus 228 (1949) 1716–1718.
- [10] H. Benoît, Théorie de l'effet Kerr d'une solution soumise à une impulsion électrique rectangulaire, Comptes Rendus 229 (1949) 30–32.
- [11] C.T. O'Konski, B.H. Zimm, New Method for Studying Electrical Orientation and Relaxation Effects in Aqueous Colloids: Preliminary Results with Tobacco Mosaic Virus. Science (80-), 111, 1950113–116, <http://dx.doi.org/10.1126/science.111.2875.113>.
- [12] C.T. O'Konski, A.J. Haltner, Electric properties of macromolecules. I. A study of electric polarization in polyelectrolyte solutions by means of electric birefringence 1, J Am Chem Soc 79 (1957) 5634–5649, <http://dx.doi.org/10.1021/ja01578a016>.
- [13] M. Tricot, C. Houssier, Electrooptical studies on sodium poly(styrenesulfonate). 1. Electric polarizability and orientation function from electric birefringence measurements, Macromolecules 15 (1982) 854–865, <http://dx.doi.org/10.1021/ma00231a032>.
- [14] S.S. Wijmenga, M. Mandel, Influence of some factors affecting the stationary value of the electric birefringence of aqueous solutions of poly(styrene sulfonates) in the presence of 0.01 mol dm<sup>-3</sup> NaCl, J Chem Soc Faraday Trans 1 Phys Chem Condens Phases 84 (1988) 2483, <http://dx.doi.org/10.1039/f19888402483>.
- [15] N. Ookubo, Y. Hirai, K. Ito, R. Hayakawa, Anisotropic counterion polarizations and their dynamics in aqueous polyelectrolytes as studied by frequency-domain electric birefringence relaxation spectroscopy, Macromolecules 22 (1989) 1359–1366, <http://dx.doi.org/10.1021/ma00193a059>.
- [16] K. Ito, A. Yagi, N. Ookubo, R. Hayakawa, Crossover behavior in high-frequency dielectric relaxation of linear polyions in dilute and semidilute solutions, Macromolecules 23 (1990) 857–862, <http://dx.doi.org/10.1021/ma00205a027>.
- [17] Y. Nagamine, K. Ito, R. Hayakawa, Low- and high-frequency electric birefringence relaxations in linear polyelectrolyte solutions †, Langmuir 15 (1999) 4135–4138, <http://dx.doi.org/10.1021/la9811564>.
- [18] F. Bordini, C. Cametti, R.H. Colby, Dielectric spectroscopy and conductivity of polyelectrolyte solutions, J Phys Condens Matter 16 (2004) R1423–R1463, <http://dx.doi.org/10.1088/0953-8984/16/49/R01>.
- [19] M. Mandel, The electric polarization of rod-like, charged macromolecules, Mol Phys 4 (1961) 489–496.
- [20] F. Oosawa, Counterion fluctuation and dielectric dispersion in linear polyelectrolytes, Biopolymers 9 (1970) 677–688, <http://dx.doi.org/10.1002/bip.1970.360090606>.
- [21] A. Minakata, N. Imai, F. Oosawa, Dielectric properties of polyelectrolytes. II. A theory of dielectric increment due to ion fluctuation by a matrix method, Biopolymers 11 (1972) 347–359, <http://dx.doi.org/10.1002/bip.1972.360110204>.
- [22] A. Warashina, A. Minakata, Dielectric properties of polyelectrolytes, IV Calculation of dielectric dispersion by a stochastic model J Chem Phys 58 (1973) 4743, <http://dx.doi.org/10.1063/1.1679053>.
- [23] G.S. Manning, Limiting laws and counterion condensation in polyelectrolyte solutions, Biophys Chem 9 (1978) 65–70, [http://dx.doi.org/10.1016/0301-4622\(78\)87016-1](http://dx.doi.org/10.1016/0301-4622(78)87016-1).
- [24] G.S. Manning, J. Ray, Fluctuations of counterions condensed on charged polymers, Langmuir 10 (1994) 962–966, <http://dx.doi.org/10.1021/la00015a058>.
- [25] G.S. Manning, A counterion condensation theory for the relaxation, rise, and frequency dependence of the parallel polarization of rodlike polyelectrolytes, Eur Phys J E Soft Matter 34 (2011) 1–7, <http://dx.doi.org/10.1140/epje/i2011-11039-2>.
- [26] J.K.G. Dhont, K. Kang, An electric-field induced dynamical state in dispersions of charged colloidal rods, Soft Matter 10 (2014) 1987–2007, <http://dx.doi.org/10.1039/c3sm52277f>.
- [27] M.E. Cates, The anomalous Kerr effect: implications for polyelectrolyte structure, J Phys II 2 (1992) 1109–1119, <http://dx.doi.org/10.1051/jp2:1992189>.
- [28] H.A. Ritacco, M. Fernández-Leyes, C. Domínguez, D. Langevin, Electric birefringence of aqueous solutions of a rigid polyelectrolyte. Polarization mechanisms and anomalous birefringence signals, Macromolecules 49 (2016) 5618–5629, <http://dx.doi.org/10.1021/acs.macromol.6b01240>.
- [29] H. Hoffmann, G. Dieter, Electric birefringence anomaly of solutions of ionically charged anisometric particles, Adv Colloid Interf Sci 216 (2015) 20–35.
- [30] F. Mantegazza, M. Caggioni, M.L. Jiménez, T. Bellini, Anomalous field-induced particle orientation in dilute mixtures of charged rod-like and spherical colloids, Nat Phys 1 (2005) 103–106, <http://dx.doi.org/10.1038/nphys124>.
- [31] G.S. Manning, Transverse polarizability of an aligned assembly of charged rods, Eur Phys J E 30 (2009) 411–415, <http://dx.doi.org/10.1140/epje/i2009-10540-5>.
- [32] X. Schlagberger, R.R. Netz, Anomalous birefringence and polarizability saturation of charged elastic rods: field-strength, salt and finite-concentration effects, EPL Europhysics Lett 83 (2008) (36003) 10.1209/0295-5075/83/36003.
- [33] F. Perrin, Mouvement brownien d'un ellipsoïde - I. Dispersion diélectrique pour des molécules ellipsoïdales, J Phys Le Radium 5 (1934) 497–511, <http://dx.doi.org/10.1051/jphysrad:01934005010049700>.
- [34] H. Hoffmann, K. Kamburova, H. Maeda, T. Radeva, Investigation of pH dependence of poly(acrylic acid) conformation by means of electric birefringence, Colloids Surfaces A Physicochem Eng Asp 354 (2010) 61–64, <http://dx.doi.org/10.1016/j.colsurfa.2009.07.032>.
- [35] L. Piculell, Understanding and exploiting the phase behavior of mixtures of oppositely charged polymers and surfactants in water, Langmuir 29 (2013) 10313–10329, <http://dx.doi.org/10.1021/la401026j>.
- [36] E.D.D. Goddard, Polymer/surfactant interaction: interfacial aspects, J Colloid Interface Sci 256 (2002) 228–235, <http://dx.doi.org/10.1006/jcis.2001.8066>.
- [37] D. Langevin, F. Monroy, Interfacial rheology of polyelectrolytes and polymer monolayers at the air-water interface, Curr Opin Colloid Interface Sci 15 (2010) 283–293, <http://dx.doi.org/10.1016/j.cocis.2010.02.002>.
- [38] K. Holmberg, Bo Jönsson, Bengt Kronberg, Björn Lindman, Surfactant-polymer systems. In: Surfactants Polym. Aqueous Solut, 2nd ed., John Wiley & Sons, New York, 2003, pp. 277–303.
- [39] Kwak JCT, C.T. Jan (Eds.), Polymer-Surfactant Systems. Surfactant Science Series, 77, M. Dekker, New York, 1998.
- [40] L. Piculell, Understanding and exploiting the phase behavior of mixtures of oppositely charged polymers and surfactants in water, Langmuir 29 (2013) 10313–10329, <http://dx.doi.org/10.1021/la401026j>.
- [41] P. Hansson, B. Lindman, Surfactant-polymer interactions, Curr Opin Colloid Interface Sci 1 (1996) 604–613, [http://dx.doi.org/10.1016/S1359-0294\(96\)80098-7](http://dx.doi.org/10.1016/S1359-0294(96)80098-7).
- [42] E.D. Goddard, K.P. Ananthapadmanabhan, Interactions of Surfactants with Polymers and Proteins, CRC Press, Boca Raton, 1993.
- [43] C.D. Bain, P.M. Claesson, D. Langevin, R. Meszaros, T. Nylander, C. Stubenrauch, et al., Complexes of surfactants with oppositely charged polymers at surfaces and in bulk, Adv Colloid Interf Sci 155 (2010) 32–49, <http://dx.doi.org/10.1016/j.cis.2010.01.007>.
- [44] B.A. Noskov, Dilational surface rheology of polymer and polymer/surfactant solutions, Curr Opin Colloid Interface Sci 15 (2010) 229–236, <http://dx.doi.org/10.1016/j.cocis.2010.01.006>.
- [45] D.J.F. Taylor, R.K. Thomas, J. Penfold, Polymer/surfactant interactions at the air/water interface, Adv Colloid Interf Sci 132 (2007) 69–110, <http://dx.doi.org/10.1016/j.cis.2007.01.002>.

- [46] P. Hansson, Interaction between polyelectrolyte gels and surfactants of opposite charge, *Curr Opin Colloid Interface Sci* 11 (2006) 351–362, <http://dx.doi.org/10.1016/j.cocis.2006.11.005>.
- [47] T. Nylander, Y. Samoshina, B. Lindman, Formation of polyelectrolyte–surfactant complexes on surfaces, *Adv Colloid Interf Sci* 123–126 (2006) 105–123, <http://dx.doi.org/10.1016/j.cis.2006.07.005>.
- [48] E. Guzmán, S. Llamas, A. Maestro, L. Fernández-Peña, A. Akanno, R. Miller, et al., Polymer–surfactant systems in bulk and at fluid interfaces, *Adv Colloid Interf Sci* 233 (2016) 38–64, <http://dx.doi.org/10.1016/j.cis.2015.11.001>.
- [49] S. Aidarova, A. Sharipova, J. Krägel, R. Miller, Polyelectrolyte/surfactant mixtures in the bulk and at water/oil interfaces, *Adv Colloid Interf Sci* 205 (2014) 87–93, <http://dx.doi.org/10.1016/j.cis.2013.10.007>.
- [50] D. Langevin, Complexation of oppositely charged polyelectrolytes and surfactants in aqueous solutions, *A Review Adv Colloid Interface Sci* 147–148 (2009) 170–177.
- [51] B.A. Noskov, G. Loglio, R. Miller, Dilational surface visco-elasticity of polyelectrolyte/surfactant solutions: formation of heterogeneous adsorption layers, *Adv Colloid Interf Sci* 168 (2011) 179–197, <http://dx.doi.org/10.1016/j.cis.2011.02.010>.
- [52] D. Langevin, Polyelectrolyte and surfactant mixed solutions. Behavior at surfaces and in thin films, *Adv Colloid Interf Sci* 89–90 (2001) 467–484, [http://dx.doi.org/10.1016/S0001-8686\(00\)00068-3](http://dx.doi.org/10.1016/S0001-8686(00)00068-3).
- [53] J.R. Lu, R.K. Thomas, J. Penfold, Surfactant layers at the air/water interface: structure and composition, *Adv Colloid Interf Sci* 84 (2000) 143–304, [http://dx.doi.org/10.1016/S0001-8686\(99\)00019-6](http://dx.doi.org/10.1016/S0001-8686(99)00019-6).
- [54] R.V. Klitzing, A. Espert, A. Asnacios, T. Hellweg, A. Colin, D. Langevin, Forces in foam films containing polyelectrolyte and surfactant, *Colloids Surfaces A Physicochem Eng Asp* 149 (1999) 131–140, [http://dx.doi.org/10.1016/S0927-7757\(98\)00307-0](http://dx.doi.org/10.1016/S0927-7757(98)00307-0).
- [55] G. Gochev, Thin liquid films stabilized by polymers and polymer/surfactant mixtures, *Curr Opin Colloid Interface Sci* 20 (2015) 115–123, <http://dx.doi.org/10.1016/j.cocis.2015.03.003>.
- [56] K. Kogej, Association and structure formation in oppositely charged polyelectrolyte-surfactant mixtures, *Adv Colloid Interf Sci* 158 (2010) 68–83, <http://dx.doi.org/10.1016/j.cis.2009.04.003>.
- [57] Lm State, Al Margolin, Sf Sherstyuk, Va Izumrudov, Ab Zezin, Va Kabanov, Enzymes in polyelectrolyte complexes, *Eur J Biochem* 146 (1985) 625–632, <http://dx.doi.org/10.1111/j.1432-1033.1985.tb08697.x>.
- [58] D.W. Deamer, The first living Systems: a bioenergetic perspective, *Microbiol Mol Biol Rev* 61 (1997) 239–261.
- [59] W. Gilbert, Origin of life: the RNA world, *Nature* 319 (1986) 618.
- [60] J. Fundin, W. Brown, Polymer/surfactant interactions. Sodium poly(styrene sulfonate) and CTAB complex formation. Light scattering measurements in dilute aqueous solution, *Macromolecules* 27 (1994) 5024–5031, <http://dx.doi.org/10.1021/ma00096a026>.
- [61] J. Xia, H. Zhang, D.R. Rigsbee, P.L. Dubin, T. Shaikh, Structural elucidation of soluble polyelectrolyte-micelle complexes: intra- vs. interpolymer association, *Macromolecules* 26 (1993) 2759–2766, <http://dx.doi.org/10.1021/ma00063a019>.
- [62] Y. Li, J. Xia, P.L. Dubin, Complex formation between polyelectrolyte and oppositely charged mixed micelles: static and dynamic light scattering study of the effect of polyelectrolyte molecular weight and concentration, *Macromolecules* 27 (1994) 7049–7055, <http://dx.doi.org/10.1021/ma00102a007>.
- [63] J.-F. Berret, B. Vigolo, R. Eng, P. Hervé, I. Grillo, L. Yang, Electrostatic self-assembly of oppositely charged copolymers and surfactants: a light, neutron, and X-ray scattering study, *Macromolecules* 37 (2004) 4922–4930, <http://dx.doi.org/10.1021/ma0498722>.
- [64] S. Trabelsi, S. Guillot, H. Ritacco, F. Boué, D. Langevin, Nanostructures of colloidal complexes formed in oppositely charged polyelectrolyte/surfactant dilute aqueous solutions, *Eur Phys J E Soft Matter* 23 (2007) 305–311, <http://dx.doi.org/10.1140/epje/i2006-10192-y>.
- [65] J.-F. Berret, G. Cristobal, P. Hervé, J. Oberdisse, I. Grillo, Structure of colloidal complexes obtained from neutral/poly- electrolyte copolymers and oppositely charged surfactants, *Eur Phys J E - Soft Matter* 9 (2002) 301–311, <http://dx.doi.org/10.1140/epje/i2002-10063-7>.
- [66] D. Li, M.S. Kelkar, N.J. Wagner, Phase behavior and molecular thermodynamics of coacervation in oppositely charged polyelectrolyte/surfactant systems: a cationic polymer JR 400 and anionic surfactant SDS mixture, *Langmuir* 28 (2012) 10348–10362, <http://dx.doi.org/10.1021/la301475s>.
- [67] M. Štěpánek, J. Hajduová, K. Procházka, M. Šlouf, J. Nebesářová, G. Mountrichas, et al., Association of poly(4-hydroxystyrene)- block -poly(ethylene oxide) in aqueous solutions: block copolymer nanoparticles with intermixed blocks, *Langmuir* 28 (2012) 307–313, <http://dx.doi.org/10.1021/la203946s>.
- [68] K. Bodnár, E. Fegyver, M. Nagy, R. Mészáros, Impact of polyelectrolyte chemistry on the thermodynamic stability of oppositely charged macromolecule/surfactant mixtures, *Langmuir* 32 (2016) 1259–1268, <http://dx.doi.org/10.1021/acs.langmuir.5b04431>.
- [69] A. Naderi, P.M. Claesson, M. Bergström, A. Dedinaite, Trapped non-equilibrium states in aqueous solutions of oppositely charged polyelectrolytes and surfactants: effects of mixing protocol and salt concentration, *Colloids Surfaces A Physicochem Eng Asp* 253 (2005) 83–93, <http://dx.doi.org/10.1016/j.colsurfa.2004.10.123>.
- [70] A. Bilalov, U. Olsson, B. Lindman, Complexation between DNA and surfactants and lipids: phase behavior and molecular organization, *Soft Matter* 8 (2012) 11022, <http://dx.doi.org/10.1039/c2sm26553b>.
- [71] E.D. Goddard, R.B. Hannan, Polymer/surfactant interactions, *J Am Oil Chem Soc* 54 (1977) 561–566, <http://dx.doi.org/10.1007/BF03027636>.
- [72] H. Ritacco, D. Kurlat, D. Langevin, Properties of aqueous solutions of polyelectrolytes and surfactants of opposite charge: surface tension, surface rheology, and electrical birefringence studies, *J Phys Chem B* 107 (2003) 9146–9158, <http://dx.doi.org/10.1021/jp034033n>.
- [73] H. Ritacco, D.H. Kurlat, Critical aggregation concentration in the PAMPS (10%)/DTAB system, *Colloids Surfaces A Physicochem Eng Asp* 218 (2003) 27–45, [http://dx.doi.org/10.1016/S0927-7757\(02\)00551-4](http://dx.doi.org/10.1016/S0927-7757(02)00551-4).
- [74] Y. Lapitsky, M. Parikh, E.W. Kaler, Calorimetric determination of surfactant/polyelectrolyte binding isotherms, *J Phys Chem B* 111 (2007) 8379–8387, <http://dx.doi.org/10.1021/jp0678958>.
- [75] K. Hayakawa, J.P. Santerre, J.C.T. Kwak, Study of surfactant-polyelectrolyte interactions. Binding of dodecyl- and tetradecyltrimethylammonium bromide by some carboxylic polyelectrolytes, *Macromolecules* 16 (1983) 1642–1645, <http://dx.doi.org/10.1021/ma00244a017>.
- [76] J. Liu, N. Takisawa, K. Shirahama, H. Abe, K. Sakamoto, Effect of polymer size on the polyelectrolyte – surfactant interaction, *J Phys Chem B* 101 (1997) 7520–7523, <http://dx.doi.org/10.1021/jp971198l>.
- [77] M. Almgren, P. Hansson, E. Mukhtar, J. Van Stam, Aggregation of alkyltrimethylammonium surfactants aqueous poly(styrenesulfonate) solutions, *Langmuir* 8 (1992) 2405–2412, <http://dx.doi.org/10.1021/la00046a011>.
- [78] E.D. Goddard, Polymer-surfactant interaction part II. Polymer and surfactant of opposite charge, *Colloids Surf A Physicochem Eng Asp* 19 (1986) 301–329, [http://dx.doi.org/10.1016/0166-6622\(86\)80341-9](http://dx.doi.org/10.1016/0166-6622(86)80341-9).
- [79] H. Diamant, D. Andelman, Self-assembly in mixtures of polymers and small associating molecules, *Macromolecules* 33 (2000) 8050–8061, <http://dx.doi.org/10.1021/ma991021k>.
- [80] P. Hansson, M. Almgren, Interaction of C nTAB with sodium (carboxymethyl)cellulose: effect of polyion linear charge density on binding isotherms and surfactant aggregation number, *J Phys Chem* 100 (1996) 9038–9046, <http://dx.doi.org/10.1021/jp953637r>.
- [81] P. Hansson, M. Almgren, Large C12TAB micelles formed in complexes with polyvinylsulfate and dextran sulfate, *J Phys Chem* 99 (1995) 16694–16703, <http://dx.doi.org/10.1021/j100045a032>.
- [82] P. Hansson, M. Almgren, Polyelectrolyte-induced micelle formation of ionic surfactants and binary surfactant mixtures studied by time-resolved fluorescence quenching, *J Phys Chem* 99 (1995) 16684–16693, <http://dx.doi.org/10.1021/j100045a031>.
- [83] P. Hansson, M. Almgren, Interaction of alkyltrimethylammonium surfactants with polyacrylate and poly(styrenesulfonate) in aqueous solution: phase behaviour and surfactant aggregation numbers, *Langmuir* 10 (1994) 2115–2124, <http://dx.doi.org/10.1021/la00019a017>.
- [84] B. Cabane, R. Duplessix, Decoration of semidilute polymer solutions with surfactant micelles, *J Phys* 48 (1987) 651–662, <http://dx.doi.org/10.1051/jphys:01987004804065100>.
- [85] T. Wallin, P. Linse, Monte Carlo simulations of polyelectrolytes at charged micelles. 1. Effects of chain flexibility, *Langmuir* 12 (1996) 305–314, <http://dx.doi.org/10.1021/la950362y>.
- [86] M. Goswami, J.M. Borreguero, P.A. Pincus, B.G. Sumpster, Surfactant-mediated polyelectrolyte self-assembly in a polyelectrolyte-surfactant complex, *Macromolecules* 48 (2015) 9050–9059, <http://dx.doi.org/10.1021/acs.macromol.5b02145>.
- [87] J. García de la Torre, Dynamic electro-optic properties of macromolecules and nanoparticles in solution: a review of computational and simulation methodologies, *Colloids Surf B: Biointerfaces* 56 (2007) 4–15, <http://dx.doi.org/10.1016/j.colsurfb.2006.10.007>.
- [88] J.G. Hernández Cifre, R. Pamies, M.C. López Martínez, J. García de la Torre, Relaxation time of non-linear polymers in dilute solution via computer simulation, *J Non-Cryst Solids* 352 (2006) 5081–5086, <http://dx.doi.org/10.1016/j.jnoncrysol.2006.01.158>.
- [89] K. Ueda, N. Iizumi, M. Sakomura, Orientation behavior of polyelectrolyte in solution under an external electric field. A coarse grain molecular dynamics simulation study, *Bull Chem Soc Jpn* 78 (2005) 430–434.
- [90] García de la Torre J, Baños FGD, H.E. Pérez Sánchez, Computational Methods for Dynamic Electro-optic Properties of Macromolecules and Nanoparticles in Solution, in: S.P. Stoylov, M. Stojmenova (Eds.), *Mol. Colloid. Electro-optics*, CRC Press, Boca Raton - London - New York, 2006, pp. 109–133, <http://dx.doi.org/10.1201/9781420009859.ch4>.
- [91] S.P. Stoylov, Colloid electro-optics electrically induced optical phenomena in disperse systems, *Adv Colloid Interf Sci* 3 (1971) 45–110, [http://dx.doi.org/10.1016/0001-8686\(71\)80002-7](http://dx.doi.org/10.1016/0001-8686(71)80002-7).
- [92] E. Fredericq, C. Houssier, *Electric Dichroism and Electric Birefringence*, Clarendon Press, Oxford, 1973.
- [93] S. Krause, *Molecular Electro-Optics. Electro-Optic Properties of Macromolecules and Colloids in Solution*, Boston, MA, Springer US, 1981 <http://dx.doi.org/10.1007/978-1-4684-3914-4>.
- [94] S.P. Stoylov, M. Stojmenova (Eds.), *Molecular and Colloidal Electro-Optics*, CRC Press. Taylor and Francis., Boca Raton - London - New York, 2006.
- [95] S.P. Stoylov, *Colloid Electro-optics: Theory, Techniques, Applications*, Academic Press, London, San Diego, New York, 1991.

- [96] E. Riande, E. Sainz, *Dipole Moments and Birefringence of Polymers*, Prentice Hall, Inc., New Jersey, 1992.
- [97] B.R. Jennings (Ed.), *Electro-Optics and Dielectrics of Macromolecules and Colloids*, Springer US, Boston, MA, 1979 <http://dx.doi.org/10.1007/978-1-4684-3497-2>.
- [98] C. Houssier, C.T. O'Konski, *Electro-Optical Instrumentation Systems with Their Data Acquisition and Treatment*. Mol. Electro-Optics, Springer US, Boston, MA, 1981 309–339, <http://dx.doi.org/10.1007/978-1-4684-3914-4.15>.
- [99] B.R. Jennings, *Introduction to Modern Electro-Optics*. Mol. Electro-Optics, Springer US, Boston, MA, 1981 27–59, <http://dx.doi.org/10.1007/978-1-4684-3914-4.2>.
- [100] H.H. Trimm, K. Parslow, B.R. Jennings, *Electric birefringence*, *J Chem Educ* 61 (1984) 1114–1118.
- [101] J.C. Bemengo, B. Roux, M. Hanss, J.C. Bemengo, B. Roux, M. Hanss, et al., *Electrical birefringence apparatus for conducting solutions*, *Rev Sci Instrum* 44 (1973) 1083–1086, <http://dx.doi.org/10.1063/1.1686306>.
- [102] J. Crossley, B.K. Morgan, M. Rujimethabhas, *New Kerr cell for low-temperature measurements*, *Rev Sci Instrum* 50 (1979) 1400–1402, <http://dx.doi.org/10.1063/1.1135715>.
- [103] N. Ookubo, *New frequency-domain electric birefringence spectrometer using an advanced digital lock-in technique*, *Rev Sci Instrum* 62 (1991) 948–956, <http://dx.doi.org/10.1063/1.1142035>.
- [104] K. Yamaoka, V. Peikov, R. Sasai, S.P. Stoylov, *Theory and experiment of reversing-pulse electric birefringence. The case of bentonite suspensions in the absence and presence of cetylpyridinium chloride*, *Colloids Surfaces A Physicochem Eng Asp* 148 (1999) 43–59, [http://dx.doi.org/10.1016/S0927-7757\(98\)00594-9](http://dx.doi.org/10.1016/S0927-7757(98)00594-9).
- [105] R. Asai, N. Ikuta, K. Yamaoka, *Reversing-pulse electric birefringence of montmorillonite particles suspended in aqueous media. Instrumentation and the effect of particle concentration, ionic strength, and valence of electrolyte on field orientation*, *J Phys Chem* 100 (1996) 17266–17275, <http://dx.doi.org/10.1021/jp961525+>.
- [106] V. Peikov, R. Sasai, S.P. Stoylov, K. Yamaoka, *Surface electric properties of the Na-bentonite cetylpyridinium chloride system as studied by reversing-pulse electric birefringence*, *J Colloid Interface Sci* 197 (1998) 78–87, <http://dx.doi.org/10.1006/jcis.1997.5255>.
- [107] H. Asai, N. Watanabe, T. Okuyama, *Reversing rectangular pulse generator applicable to transient electric birefringence*, *Rev Sci Instrum* 49 (1978) 236–237, <http://dx.doi.org/10.1063/1.1135374>.
- [108] D.N. Holcomb, I. Tinoco, *Electrical birefringence at high fields 1*, *J Phys Chem* 67 (1963) 2691–2698, <http://dx.doi.org/10.1021/j100806a044>.
- [109] T. Troppenz, A. Kuijk, A. Imhof, A. van Blaaderen, M. Dijkstra, R. van Roij, et al., *Nematic ordering of polarizable colloidal rods in an external electric field: theory and experiment*, *Phys Chem Chem Phys* 17 (2015) 22423–22430, <http://dx.doi.org/10.1039/C5CP01478F>.
- [110] S. Ogawa, S. Oka, *Theory of electric birefringence in dilute solutions of tobacco mosaic virus*, *J Phys Soc Japan* 15 (1960) 658–668, <http://dx.doi.org/10.1143/JPSJ.15.658>.
- [111] G. Thurston, D. Bowling, *The frequency dependence of the Kerr effect for suspensions of rigid particles*, *J Colloid Interface Sci* 30 (1969) 34–45, [http://dx.doi.org/10.1016/0021-9797\(69\)90376-2](http://dx.doi.org/10.1016/0021-9797(69)90376-2).
- [112] H. Watanabe, A. Morita, *Kerr effect relaxation in high electric fields*, in: I. Prigogine, S.A. Rice (Eds.), *Adv. chem. physics*, 56, John Wiley & Sons, Inc., 1984, pp. 255–409, <http://dx.doi.org/10.1002/9780470142806.ch3>.
- [113] A. Peterlin, H.A. Stuart, *Über die Bestimmung der Größe und Form, sowie der elektrischen, optischen und magnetischen Anisotropie von submikroskopischen Teilchen mit Hilfe der künstlichen Doppelbrechung und der inneren Reibung*, *Zeitschrift Für Phys* 112 (1939) 129–147, <http://dx.doi.org/10.1007/BF01340060>.
- [114] J.-L. Déjardin, *Dynamic Kerr effect: the use and limits of the Smoluchowski equation and nonlinear responses*, World Scientific Publishing Co. Pte. Ltd., Singapore, 1995.
- [115] S. Krause, C.T. O'Konski, *Electric birefringence dynamics*. Mol. Electro-Optics, Springer US, Boston, MA, 1981 147–162, <http://dx.doi.org/10.1007/978-1-4684-3914-4.7>.
- [116] I.J. Tinoco, K. Yamaoka, *The reversing pulse technique in electric birefringence*, *J Phys Chem* 63 (1959) 423–427.
- [117] C.T. O'Konski, K. Yoshioka, W.H. Orttung, *Electric properties of macromolecules. IV. Determination of electric and optical parameters from saturation of electric birefringence in solutions*, *J Phys Chem* 63 (1959) 1558–1565, <http://dx.doi.org/10.1021/j150580a004>.
- [118] M. Matsumoto, H. Watanabe, K. Yoshioka, *The transient electric birefringence of rigid macromolecules in solution under the action of a rectangular pulse and a reversing pulse*, *J Phys Chem* 74 (1970) 2182–2188, <http://dx.doi.org/10.1021/j100909a025>.
- [119] G. Koopmans, J. de Boer, J. Greve, *Transient electric birefringence of macromolecular solutions*, in: B.R. Jennings (Ed.), *Electro-optics dielectr. Macromol. Colloids*, Springer US, Boston, MA, 1979, pp. 13–19.
- [120] R.J. Lewis, R. Pecora, D. Eden, *Transient electric birefringence measurements of the rotational and internal motions of a 1010 base pair DNA fragment - field strength and pulse length effects*, *Macromolecules* 20 (1987) 2579–2587, <http://dx.doi.org/10.1021/ma00176a044>.
- [121] N.V.V. Tsvetkov, M.E.E. Mikhailova, E.V.V. Lebedeva, A.A.A. Lezov, V.B.B. Rogozhin, T.A.A. Rotinyan, *Influence of the strength of polarizing electric field on free relaxation of electric birefringence in poly(butyl-isocyanate) solutions*, *Chem Phys Lett* 648 (2016) 137–142, <http://dx.doi.org/10.1016/j.cplett.2016.02.017>.
- [122] R.L. Jernigan, S. Miyazawa, *Kerr effects of flexible macromolecules*. In: *Mol. Electro-Optics*, Springer US, Boston, MA, 1981, pp. 163–179, <http://dx.doi.org/10.1007/978-1-4684-3914-4.8>.
- [123] A.V. Dobrynin, M. Rubinstein, *Theory of polyelectrolytes in solutions and at surfaces*, *Prog Polym Sci* 30 (2005) 1049–1118.
- [124] V. Degiorgio, F. Mantegazza, R. Piazza, *Transient electric birefringence measurement of the persistence length of sodium polystyrene sulfonate*, *Europhys Lett* 15 (1991) 75–80, <http://dx.doi.org/10.1209/0295-5075/15/1/013>.
- [125] V. Degiorgio, T. Bellini, F. Mantegazza, *Measurements of the persistence length of flexible polyelectrolytes*, *Int J Polym Anal Charact* 2 (1995) 83–93, <http://dx.doi.org/10.1080/10236669508233897>.
- [126] V. Degiorgio, T. Bellini, R. Piazza, F. Mantegazza, R. Goldstein, *Stretched-exponential relaxation of electric birefringence in polymer solutions*, *Phys Rev Lett* 64 (1990) 1043–1046, <http://dx.doi.org/10.1103/PhysRevLett.64.1043>.
- [127] P.J. Hagerman, B.H. Zimm, *Monte Carlo approach to the analysis of the rotational diffusion of wormlike chains*, *Biopolymers* 20 (1981) 1481–1502, <http://dx.doi.org/10.1002/bip.1981.360200709>.
- [128] P.J. Hagerman, *Investigation of the flexibility of DNA using transient electric birefringence*, *Biopolymers* 20 (1981) 1503–1535, <http://dx.doi.org/10.1002/bip.1981.360200710>.
- [129] A. Ortega, Torre J. Garcia de la, *Hydrodynamic properties of rodlike and disklike particles in dilute solution*, *J Chem Phys* 119 (2003) 9914–9919, <http://dx.doi.org/10.1063/1.1615967>.
- [130] W.A. Wegene, F.R.M. Dowben, V.J. Koester, *Time-dependent birefringence, linear dichroism, and optical rotation resulting from rigid-body rotational diffusion*, *J Chem Phys* 70 (1979) 622, <http://dx.doi.org/10.1063/1.437541>.
- [131] S. Broersma, *Rotational diffusion constant of a cylindrical particle*, *J Chem Phys* 32 (1960) 1626–1631.
- [132] Sánchez H.E. rez, J.G. De La Torre, Baños FGD, *Transient electric birefringence of wormlike macromolecules in electric fields of arbitrary strength: a computer simulation study*, *J Chem Phys* 122 (2005) 124902, <http://dx.doi.org/10.1063/1.1863892>.
- [133] N. Imai, T. Onishi, *Analytical solution of Poisson-Boltzmann equation for two-dimensional many-center problem*, *J Chem Phys* 30 (1959) 1115–1116, <http://dx.doi.org/10.1063/1.1730112>.
- [134] F. Oosawa, *Polyelectrolytes*. first, Marcel Dekker, New York, 1971.
- [135] G.S. Manning, *Limiting laws and counterion condensation in polyelectrolyte solutions I, Colligative Properties* *J Chem Phys* 51 (1969) 924, <http://dx.doi.org/10.1063/1.1672157>.
- [136] G.S. Manning, *Limiting laws and counterion condensation in polyelectrolyte solutions II, Self-Diffusion of the Small Ions* *J Chem Phys* 51 (1969) 934, <http://dx.doi.org/10.1063/1.1672158>.
- [137] G.S. Manning, *Polyelectrolytes*, *Annu Rev Phys Chem* 23 (1972) 117–140, <http://dx.doi.org/10.1146/annurev.pc.23.100172.001001>.
- [138] M. Fixman, *Charged macromolecules in external fields. I The sphere* *J Chem Phys* 72 (1980) 5177–5186, <http://dx.doi.org/10.1063/1.439753>.
- [139] M. Fixman, *Charged macromolecules in external fields. 2. preliminary remarks on the cylinder*, *Macromolecules* 13 (1980) 711–716, <http://dx.doi.org/10.1021/ma60075a043>.
- [140] W. Van Dijk, F. Van Der Touw, M. Mandel, *Influence of counterion exchange on the induced dipole moment and its relaxation for a rodlike polyon*, *Macromolecules* 14 (1981) 792–795, <http://dx.doi.org/10.1021/ma50004a062>.
- [141] A. Morita, H. Watanabe, *Dynamic behavior of the induced polarization arising from the motion of counterions bound on a rodlike polyon*, *Macromolecules* 17 (1984) 1545–1550, <http://dx.doi.org/10.1021/ma00138a021>.
- [142] J.K.G. Dhont, K. Kang, *Electric-field-induced polarization of the layer of condensed ions on cylindrical colloids*, *Eur Phys J E Soft Matter* 34 (2011) 1–19, <http://dx.doi.org/10.1140/epje/i2011-11040-9>.
- [143] K. Yamaoka, M. Tanigawa, R. Sasai, *Reversing-pulse electric birefringence of disklike suspension in the low electric field region: an extension of the ion-fluctuation model*, *J Chem Phys* 101 (1994) 1625–1631, <http://dx.doi.org/10.1063/1.467783>.
- [144] K. Yamaoka, R. Sasai, K. Kohno, *Low-field expressions for reversing-pulse electric birefringence of ionized polyions with permanent, ionic, and electronic dipole moments: a further extension of the ion-fluctuation theory and the application to poly( $\alpha$ , L-glutamic acid)*, *J Chem Phys* 105 (1996) 8958–8964, <http://dx.doi.org/10.1063/1.472733>.
- [145] A. Szabo, M. Haleem, D. Eden, *Theory of the transient electric birefringence of rod-like polyions: coupling of rotational and counterion dynamics*, *J Chem Phys* 85 (1986) 7472–7479, <http://dx.doi.org/10.1063/1.451336>.
- [146] H. Takezoe, H. Yu, *Dynamic kerr effect measurements on photoreceptor disk membrane vesicles*, *Biophys Chem* 13 (1981) 49–54, [http://dx.doi.org/10.1016/0301-4622\(81\)80024-5](http://dx.doi.org/10.1016/0301-4622(81)80024-5).
- [147] H. Takezoe, H. Yu, *Lateral diffusion of photopigments in photoreceptor disk membrane vesicles by the dynamic Kerr effect*, *Biochemistry* 20 (1981) 5275–5281, <http://dx.doi.org/10.1021/bi00521a028>.
- [148] H.A. Ritacco, D. Kurlat, R.G. Rubio, F. Ortega, D. Langevin, *Stationary electric birefringence of flexible polyelectrolyte solutions: experimental evidence of different Counterion polarization mechanisms*, *Macromolecules* 42 (2009) 5843–5850, <http://dx.doi.org/10.1021/ma900438u>.
- [149] S. Sotkerov, G. Weill, *Polarized fluorescence in an electric field: steady state and transient values for the fourth moment of the orientation function at arbitrary*

- fields, *Biophys Chem* 10 (1979) 41–46, [http://dx.doi.org/10.1016/0301-4622\(79\)80004-6](http://dx.doi.org/10.1016/0301-4622(79)80004-6).
- [150] S. Diekmann, W. Hillen, M. Jung, R.D. Wells, D. Pörschke, Electric properties and structure of DNA-restriction fragments from measurements of the electric dichroism, *Biophys Chem* 15 (1982) 157–167, [http://dx.doi.org/10.1016/0301-4622\(82\)80028-8](http://dx.doi.org/10.1016/0301-4622(82)80028-8).
- [151] D. Pörschke, C. Créminon, X. Cousin, C. Bon, J. Sussman, I. Silman, Electrooptical measurements demonstrate a large permanent dipole moment associated with acetylcholinesterase, *Biophys J* 70 (1996) 1603–1608, [http://dx.doi.org/10.1016/S0006-3495\(96\)79759-X](http://dx.doi.org/10.1016/S0006-3495(96)79759-X).
- [152] K. Yoshioka, Orientation function of the electric birefringence and dichroism of rodlike polyelectrolytes on the basis of the saturating dipole mechanism, *J Chem Phys* 79 (1983) 3482–3486, <http://dx.doi.org/10.1063/1.446199>.
- [153] N.C. Stellwagen, Electric birefringence of restriction enzyme fragments of DNA: optical factor and electric polarizability as a function of molecular weight, *Biopolymers* 20 (1981) 399–434, <http://dx.doi.org/10.1002/bip.1981.360200302>.
- [154] S. Stoylov, Polar Nanoparticles, in: S.P. Stoylov, M. Stoimenova (Eds.), *Mol. Colloid. Electro-optics*, CRC Press, Boca Raton - London- New York, 2006, pp. 17–38, <http://dx.doi.org/10.1201/9781420009859.pt1>.
- [155] S.P. Stoylov, Electro-optical investigations of the dipole moments of nanoparticles, *Colloids Surf B: Biointerfaces* 56 (2007) 50–58, <http://dx.doi.org/10.1016/j.colsurfb.2006.11.016>.
- [156] H. Washizu, K. Kikuchi, Simulation of electric polarizability of polyelectrolytes, in: S.P. Stoylov, M. Stoimenova (Eds.), *Mol. Colloid. Electro-optics*, CRC Press, Boca Raton - London- New York, 2006, pp. 135–147, <http://dx.doi.org/10.1201/9781420009859.ch5>.
- [157] H.A. Stuart, A. Peterlin, Optische Anisotropie und Form von Fadenmolekülen, II Künstliche Doppelbrechung *J Polym Sci* 5 (1950) 551–563, <http://dx.doi.org/10.1002/pol.1950.120050503>.
- [158] D.A. Dows, Kerr effect in flexible polymers, *J Chem Phys* 41 (1964) 2656–2660, <http://dx.doi.org/10.1063/1.1726333>.
- [159] K. Nagai, T. Ishikawa, Internal rotation and Kerr effect in polymer molecules, *J Chem Phys* 43 (1965) 4508–4515, <http://dx.doi.org/10.1063/1.1696725>.
- [160] P.J. Flory, R.L. Jernigan, Kerr effect in polymer chains, *J Chem Phys* 48 (1968) 3823–3824, <http://dx.doi.org/10.1063/1.1669691>.
- [161] P.J. Flory, Foundations of rotational isomeric state theory and general methods for generating configurational averages, *Macromolecules* 7 (1974) 381–392, <http://dx.doi.org/10.1021/ma60039a022>.
- [162] S.S. Wijmenga, M. Mandel, The electric polarizability and the Kerr constant of a gaussian charged polyelectrolyte chain in solution, *J Mol Liq* 36 (1987) 119–133, [http://dx.doi.org/10.1016/0167-7322\(87\)80035-1](http://dx.doi.org/10.1016/0167-7322(87)80035-1).
- [163] P.J. Rudd, B.R. Jennings, Electric birefringence for the study of polymer-surfactant interactions. The polyvinylpyrrolidone-sodium dodecyl sulphate system, *J Colloid Interface Sci* 48 (1974) 302–306, [http://dx.doi.org/10.1016/0021-9797\(74\)90164-7](http://dx.doi.org/10.1016/0021-9797(74)90164-7).
- [164] Y. Wu, J. Chen, Y. Fang, M. Zhu, Polyvinylpyrrolidone-sodium dodecylsulfate complex is a family of pseudo-polyanions with different charge densities: evidence from capillary electrophoresis, capillary viscosimetry and conductometry, *J Colloid Interface Sci* 479 (2016) 34–42, <http://dx.doi.org/10.1016/j.jcis.2016.06.037>.
- [165] A.K. Wright, M.R. Thompson, R.L. Miller, A study of protein-sodium dodecyl sulfate complexes by transient electric birefringence, *Biochemistry* 14 (1975) 3224–3228, <http://dx.doi.org/10.1021/bi00685a030>.
- [166] E.S. Rowe, J. Steinhardt, Electrooptical properties of reduced protein-sodium dodecyl sulfate complexes, *Biochemistry* 15 (1976) 2579–2585, <http://dx.doi.org/10.1021/bi00657a015>.
- [167] R. Fairey, B. Jennings, Electrooptical study of the effect of surfactant on attapulgite clay sol stability, *J Colloid Interface Sci* 85 (1982) 205–215, [http://dx.doi.org/10.1016/0021-9797\(82\)90249-1](http://dx.doi.org/10.1016/0021-9797(82)90249-1).
- [168] G.S. Manning, Ionic polarizability of interacting charged rods, *EPL Europhysics Lett* 86 (2009) (36001) 10.1209/0295-5075/86/36001.
- [169] F.P. Cavalino, H. Hoffmann, C. Sbriziolo, M.L. Turco Liveri, Interactions of tetradecyldimethylaminoxide with polyacrylic and polymethacrylic acids in aqueous solution, *Colloids Surfaces A Physicochem Eng Asp* 183–185 (2001) 689–697, [http://dx.doi.org/10.1016/S0927-7757\(01\)00495-2](http://dx.doi.org/10.1016/S0927-7757(01)00495-2).
- [170] A.R. Foweraker, M. Isles, B.R. Jennings, T.E. Hardingham, H. Muir, Electric birefringence studies of cartilage proteoglycan aggregation, *Biopolymers* 16 (1977) 1367–1369, <http://dx.doi.org/10.1002/bip.1977.360160617>.
- [171] M. Isles, A.R. Foweraker, B.R. Jennings, T. Hardingham, H. Muir, Characterization of proteoglycan and the proteoglycan–hyaluronic acid complex by electric birefringence, *Biochem J* 173 (1978) 237–243, <http://dx.doi.org/10.1042/bj1730237>.
- [172] E.Y. Hawkins, A.R. Foweraker, B.R. Jennings, Analysis of multicomponent electric birefringence transients: data for proteoglycan solutions, *Polymer (Guildf)* 19 (1978) 1233–1236, [http://dx.doi.org/10.1016/0032-3861\(78\)90080-0](http://dx.doi.org/10.1016/0032-3861(78)90080-0).
- [173] D.C. Rau, E. Charney, Electric dichroism of DNA, *Biophys Chem* 17 (1983) 35–50, [http://dx.doi.org/10.1016/0301-4622\(83\)87012-4](http://dx.doi.org/10.1016/0301-4622(83)87012-4).
- [174] D. Pörschke, The mechanism of ion polarisation along DNA double helices, *Biophys Chem* 22 (1985) 237–247, [http://dx.doi.org/10.1016/0301-4622\(85\)80046-6](http://dx.doi.org/10.1016/0301-4622(85)80046-6).
- [175] M. Pollak, H.A. Glick, Evidence for electrically induced partial strand separation of DNA, *Biopolymers* 16 (1977) 1007–1013, <http://dx.doi.org/10.1002/bip.1977.360160505>.
- [176] S. Diekmann, W. Hillen, B. Morgeneyer, R.D. Wells, D. Pörschke, Orientation relaxation of DNA restriction fragments and the internal mobility of the double helix, *Biophys Chem* 15 (1982) 263–270, [http://dx.doi.org/10.1016/0301-4622\(82\)80009-4](http://dx.doi.org/10.1016/0301-4622(82)80009-4).
- [177] P.J. Hagerman, Evidence for the existence of stable curvature of DNA in solution, *Proc Natl Acad Sci* 81 (1984) 4632–4636.
- [178] N. Ise, M. Eigen, G. Schwarz, The orientation and dissociation field effect of DNA in solution, *Biopolymers* 1 (1963) 343–352, <http://dx.doi.org/10.1002/bip.360010406>.
- [179] C.T. O'Konski, N.C. Stellwagen, Structural transition produced by electric fields in aqueous sodium Deoxyribonucleate, *Biophys J* 5 (1965) 607–613, [http://dx.doi.org/10.1016/S0006-3495\(65\)86737-6](http://dx.doi.org/10.1016/S0006-3495(65)86737-6).
- [180] K. Yamaoka, K. Matsuda, Electric dipole moments of DNA in aqueous solutions as studied by the reversing-pulse electric birefringence, *Macromolecules* 13 (1980) 1558–1560, <http://dx.doi.org/10.1021/ma60078a037>.
- [181] S. Takashima, Optical anisotropy of synthetic polynucleotides. I. Flow birefringence and  $\pi$ -electron polarizability of bases, *Biopolymers* 6 (1968) 1437–1452, <http://dx.doi.org/10.1002/bip.1968.360061007>.
- [182] R.J. Lewis, R. Pecora, D. Eden, Transient electric birefringence measurements of the rotational and internal bending modes in monodisperse DNA fragments, *Macromolecules* 19 (1986) 134–139, <http://dx.doi.org/10.1021/ma00155a021>.
- [183] N. Jain, S. Trabelsi, S. Guillot, D. McLoughlin, D. Langevin, P. Letellier, et al., Critical aggregation concentration in mixed solutions of anionic polyelectrolytes and cationic surfactants, *Langmuir* 20 (2004) 8496–8503, <http://dx.doi.org/10.1021/la0489918>.
- [184] T. Radeva, V. Milkova, I. Petkanchin, Electrical properties of multilayers from low- and high-molecular-weight polyelectrolytes, *J Colloid Interface Sci* 279 (2004) 351–356, <http://dx.doi.org/10.1016/j.jcis.2004.06.078>.
- [185] T. Radeva, V. Milkova, I. Petkanchin, Dynamics of counterions in polyelectrolyte multilayers studied by electro-optics, *Colloids Surfaces A Physicochem Eng Asp* 240 (2004) 27–34, <http://dx.doi.org/10.1016/j.colsurfa.2004.03.010>.
- [186] T. Radeva, V. Milkova, I. Petkanchin, Structure and electrical properties of polyelectrolyte multilayers formed on anisometric colloidal particles, *J Colloid Interface Sci* 244 (2001) 24–30, <http://dx.doi.org/10.1006/jcis.2001.7815>.
- [187] T. Radeva, V. Milkova, I. Petkanchin, Electro-optics of colloids coated with multilayers from strong polyelectrolytes: surface charge relaxation, *J Colloid Interface Sci* 266 (2003) 141–147, [http://dx.doi.org/10.1016/S0021-9797\(03\)00533-2](http://dx.doi.org/10.1016/S0021-9797(03)00533-2).
- [188] T. Radeva, K. Kamburova, Electro-optics of colloid-polyelectrolyte complexes: counterion release from adsorbed macromolecules, *J Colloid Interface Sci* 293 (2006) 290–295, <http://dx.doi.org/10.1016/j.jcis.2005.06.066>.
- [189] T. Radeva, M. Grozeva, In situ determination of thickness and electrical properties of multilayers from weak polyelectrolytes, *J Colloid Interface Sci* 287 (2005) 415–421, <http://dx.doi.org/10.1016/j.jcis.2005.02.016>.